2012

Design and Development of a Low Cost and Lightweight Laser Rangefinder

Miguel Lopez
CUNY City College

Design and Development of a Low Cost and Lightweight Laser Rangefinder

THESIS

Submitted in partial fulfillment towards the degree of
Master of Science in Electrical Engineering
At
The City College of the City University of New York

Submitted by: **Miguel Lopez**
May 2012

Approved by:

_____	_____
Professor Jizhong Xiao, Advisor Department of Electrical Engineering The City College of New York	Professor Roger Dorsinville, Chairman Department of Electrical Engineering The City College of New York

Table of Contents

ACKNOWLEDGEMENTS.....III
ABSTRACT.....IV
LIST OF TABLES.....V
LIST OF FIGURES.....V
Chapter I. Introduction.....1
Chapter II. Design Theory and Specification.....2
2.1. Sending Channel Hardware..... 2
2.1.1. Microcontroller Unit.....2
2.1.2. Laser Diode Driver.....2
2.2. Receiver Channel Hardware.....3
2.2.1. Time of Flight Calculation..... 3
2.2.2. High Voltage Power Supply.....3
2.2.3. Pre- and Post-Amplifiers.....3
2.2.4. Optical Lens.....4
Chapter III. Design Implementation.....5
3.1. Sending Channel Hardware.....6
3.1.1. Microcontroller.....6
3.1.2. Pulsed Laser Diode and Driver Circuit.....7
3.2. Receiver Channel Hardware.....8
3.2.1. Time to Digital Converter.....8
3.2.1.1. Key Features..... 9
3.2.1.2. Microcontroller Interface.....9
3.2.1.3. Measurement Range Mode.....9
3.2.2. High Voltage Power Supply.....10
3.2.3. Current to Voltage Converter and Amplifier.....11
3.2.4. Signal Discriminator.....20
3.3. PCB Design.....21
Chapter IV. System Testing.....22
4.1. Microcontroller-TDC Interface.....23
4.2. Distance Measurement.....24
Chapter V. System Improvements and Conclusion.....26
5.1. Sending Channel Improvement.....26
5.2. Receiver Channel Improvement.....27
5.3. Conclusion.....28
Bibliography.....30

ACKNOWLEDGEMENTS

First, I would like to thank Prof. Jizhong Xiao for providing me with the opportunity to work on such interesting research which allows me to learn and expand my research experiences in the fields of Digital and Analog Design. Furthermore, I would like to express my deepest gratitude to Prof. Xiao for the guidance and support provided throughout the years.

Also, I am very grateful for being financially supported by the Louis Strokes Alliance for Minority Participation (LSAMP)'s Bridge to the Doctorate Program (BTD) throughout my research. At the BTD's office, I would like to thank Prof. Claude Brathwaite for always believing in me and giving me positive support and guidance.

I would like to extend my thanks to Prof. Song Qiang for all his positive inputs throughout the project. Moreover, I am thankful to Prof. Song for taking time to teach me the software I needed in order to complete my design.

I would also like to thank my colleagues: Carlos Jaramillo for helping me with the mechanical design, Ivan Dryanovski, William Morris, Samleo Joseph and Roberto Valenti for their valuable technical inputs during this project.

Last but not least, I would like to thank my family for all their emotional support, especially to my fiancé Yaneiry Jaquez.

Design and Development of a Low Cost and Lightweight Laser Rangefinder

By Miguel Lopez

Submitted to the Department of Electrical Engineering of City College of New York
On May 21, 2012, in partial fulfillment of the requirements for the degree of
Master of Engineering in Electrical Engineering

Abstract:

The purpose of this work is to design, develop and test integrated electronics and optoelectronic circuits comprised of devices that can yield a low cost and lightweight pulsed time-of-flight laser rangefinder. The pulsed laser rangefinder measures distances of up to 60-meters, provides a low power consumption, fast speed, and lightweight. The design implemented measures the range information based on the time taken for a light pulse to reach a target and echo back. This design comprised of a light emitting circuit that outputs short and powerful pulses of laser beam toward a measurement target object; a light receiving circuit that photo-electrically converts the laser light reflected from the target object and amplifies the converted optical signal; a time to digital converter (TDC) to calculate the TOF of the laser light; and a microprocessor which is used for system control, distance calculation, and synchronization with the host computer. The design presented here is implemented in such a way that it allows its expendability to a 2D scanning laser rangefinder without major changes. Expanding the system to a 2D scanning laser rangefinder will help to improve autonomous robots abilities of building a map of an unknown environment, navigation, object avoidance and qualification.

Thesis Supervisor: Prof. Jizhong Xiao

List of Tables

Table 1 Transimpedance amplifiers feedback pole values....12
Table 2 Transimpedance amplifiers Feedback capacitor values....12
Table 3 Transimpedance amplifiers -3dB computed bandwidth values....13
Table 4 TDC-GP1 testing measurements....23
Table 5 Time of flight measurements....24

List of Figures

Figure 1 Block diagram of a pulsed laser rangefinder....1
Figure 2.1 Transimpedance amplifier equivalent circuit....4
Figure 2.2 Optical collimating lens....4
Figure 2.3 C170TME mounted aspherical lens from Thorlabs, INC....5
Figure 2.4 Optical receiving lens....6
Figure 3.1 Block diagramof the laser rangefinder electronics....6
Figure 3.2 Block diagram of the ATMega128....7
Figure 3.3 Pulsed laser diode driver....8
Figure 3.4 TDC-GP1 pinout....9
Figure 3.5 5V to 200V DC-DC converter for APD bias....10
Figure 3.6 High voltage DC-DC converter....11
Figure 3.7 Transimpedance amplifier circuit using the OPA657....14
Figure 3.8 Transimpedance amplifier circuit using the OPA656....14
Figure 3.9 Output noise of the transimpedance amplifier using the OPA657....15
Figure 3.10 Input noise of the transimpedance amplifier using the OPA657....15
Figure 3.11 Total noise of the transimpedance amplifier using the OPA657....16
Figure 3.12 Output noise of the transimpedance amplifier using the OPA656....16
Figure 3.13 Input noise of the transimpedance amplifier using the OPA656....17
Figure 3.14 Total noise of the transimpedance amplifier using the OPA656....17
Figure 3.15 OPA656 filtered noise signal....18
Figure 3.16 Receiver channel amplifying circuit....18
Figure 3.17 DC tranfer characteristic of the amplifying circuit....19
Figure 3.18 Output noise of the amplifying circuit....19
Figure 3.19 Input noise of the amplifying circuit....20
Figure 3.20 Total noise generated by the amplifying circuit....20
Figure 3.21 LT1016 voltage comparator....21
Figure 3.22 PCB of laser rangefinder....22
Figure 3.23 Unpopulated rangefinder board....22
Figure 3.24 Populated rangefinder board....22
Figure 4.1 ATMega128 and TDC-GP1 interface....23
Figure 4.2 Time measured at different reference distances....25
Figure 4.3 Average time measured at different reference distances....26
Figure 5.1 Average time measured at cooler temperature....27
Figure 5.2 Thermoelectric controller....28
Figure 5.3 Principle of time domain compensation....29

1. Introduction

Today's societal needs require a more holistic approach to engineering design. Keeping in mind the demand of a more sustainable environment, the purpose of this research is to design and develop a low cost and lightweight pulsed laser rangefinder that could measure distances of up to 60-meters. Pulsed Laser rangefinders are high resolution systems used to measure targets whose distance ranges from centimeters to kilometers. A pulsed laser rangefinder operates on the time-of-flight (TOF) principle which measures the flight time (delay time) of a light from a pulsed laser to be reflected off the target and back to the receiver. By measuring the TOF of the laser signal, the range can be determined since the value of the speed of light is well established. The advantage of a pulsed TOF method over many other distance measurement methods, such as triangulation or phase modulation, is that unambiguous centimeter-level accuracy is already available in a single measurement [3]-[5].This principle is shown in Figure 1.

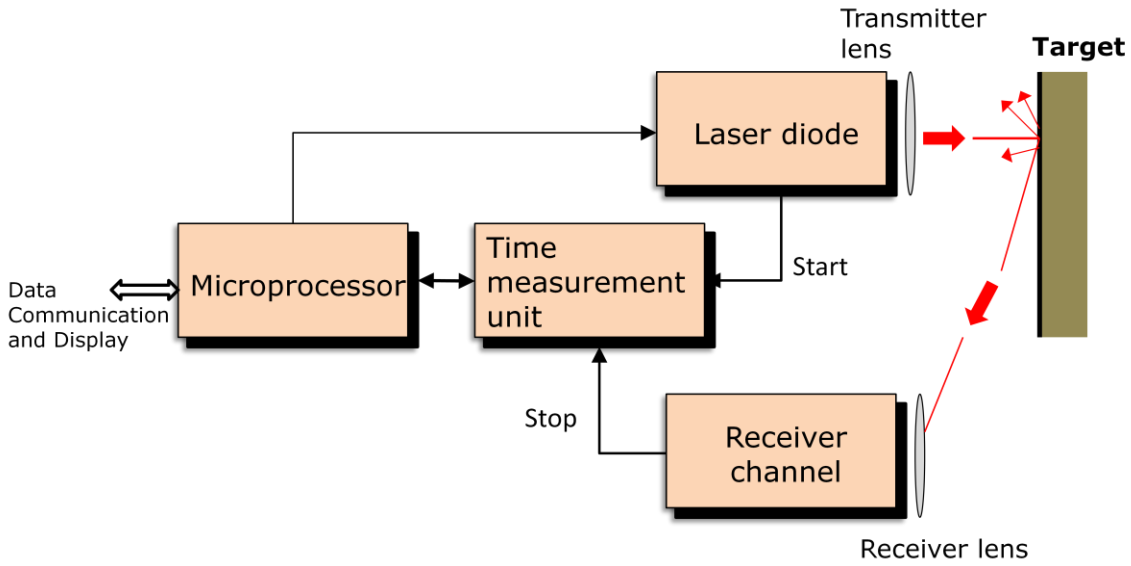

Figure 1.1 Block Diagram of a Pulsed Laser Rangefinder

This type of distance measuring apparatus is used in a variety of application such as:

- The military to measure long distances.
- Robots visual sensors or an automatic guided vehicle.
- The construction industry as digital measuring tape.
- Safety sensor to measure a person proximity to dangerous equipments.
- To measure height of small aerial vehicles.

Typically, pulsed TOF laser rangefinders are composed of:

- A light emitting circuit- this circuit contains a pulsed laser diode (PLD) as a light source, and a driving circuit for driving the PLD and outputting a light pulsed measurement of several nano-seconds.
- A light receiver circuit- this circuit includes an avalanche photodiode (APD) for photo-electrically convert the received light; a high voltage source to bias the APD; and an amplifying system for impedance converting and amplifying the reflected signal photo-electrically converted by the APD.
- Time measurement unit – this is composed of a time to digital converter (TDC) which is used to measure the TOF of the emitted laser beam.
- Microprocessor- this is used to calculate the distance and system control.

The design presented on this paper measures distances by sending a fire signal to the driving circuit of the PLD. This signal also serves as the START counter signal for the TDC. After the light is reflected from the measurement target, it is focused on an APD and the nano-amp level of current generated by the APD is amplified to a TTL voltage level which serves as the STOP mark for the time measurement unit by means of a leading edge discriminator. After the TDC calculates the TOF of the laser signal, the time information is read by the microprocessor which calculates the distance using the formula: $D = {}^{ct}/_{2}$ where *D* is the target distance, *c* is the speed of light, and *t* is time. The long term of this work is to implement a 2D scanning laser rangefinder and later a 3D scanning laser rangefinder. Therefore, the design presented here will be implemented in a way that it could be customized to implement a scanning laser rangefinder by adding a system of rotating mirrors and encoders to the implementation [6].

2. Design Theory and Specification

This chapter derives a set of the steps taken toward the design of the sending and receiving channels of the laser rangefinder. The chapter then goes on to a breakdown of each of the subsystems in these channels and detail the theory of operation of each subsystem as well as the design considerations taken into consideration for the design of each subsystem.

2.1. Sending Channel Hardware

This section describes how the laser light sending circuit must be implemented. The sending channel fires a short and powerful pulse of light toward a measurement target object. The light projector circuit contains a light emitting device such as a pulsed laser diode (PLD) and a PLD driving device. The nano-seconds driving pulses are sent from a microcontroller.

2.1.1. Microcontroller Unit

This section outlines the functions of the microcontroller in the operation of the laser rangefinder. The main function of the microcontroller is to record the time measurement from the time-measuring unit, average the time measurements and calculate the distance. After the distance is calculated, the data is transmitted to a PC.

The microcontroller sends the signals to start the counter for the time measurement unit and to send the laser light pulse. Also, the microcontroller is used to initiate and set the parameters of the time measurement unit (speed, mode, resolution, etc.) After the time measurement unit calculates the time, the microcontroller reads and stores the time information. At least fifty time measurements are taken from each distance to be measured. The more samples taken the most accurate the results are, but the more time needed to obtain the distance measurement.

Once the microcontroller has obtained the values for the time and computes their average, it calculates the distance value and transmits it to a PC using USART interface. Each distance calculation should take less than 20ms. This time depends on the number of time measurements taken and the duty factor of the pulse laser diode.

2.1.2. Laser Diode Driver

This section outlines the function of the laser driver. The main function of this driver is to provide fast, high current pulses to drive the PLD. The PLD is operated in a short pulse mode in order to achieve high peak powers with fast rise and fall times.

The design of the driver is relatively easy but some considerations must be taken in consideration due to the sensitivity of the PLDs. The frequency of the pulse must match the duty factor of the PLD which is around 0.1% (ex. a 100ns current pulse must be follow by a 100µs pause). Having a higher duty factor will deteriorate and damage the PLD. Furthermore, the pulse duration should be less than 1µs.

The amount of current generated by the driver must be limited not to exceed the maximum forward current of the PLD. Most PLDs found have a beam divergence from 12◦ to 25◦ parallel to the pn-junction. In order to maximize the optical power of the PLD, a collimating lens is used to minimize the divergence of the laser beam. This is explained in more details in the following sections.

2.2. Receiving Channel Hardware

A small fraction of the light beam emitted by the PLD is received by an optical receiver and focus on the APD which photo-electrically convert the pulse of light received. The small pulse of current generated by the APD is converted into a TTL voltage level signal using a two-stage transimpedance amplifier. This voltage signal serves as the STOP signal for the time counter.

2.2.1. Time of Flight Calculation

As mentioned above, the method of rangefinder used in this design is the TOF. To measure the time of flight of the emitted pulsed of light, an ultra-fast counter as a TDC is used. TDCs are used to measure the time intervals between two events with a resolution of less than one nanosecond.

The accuracy of a pulsed TOF laser radar depends critically on the performance of its time measurement unit [18]. Therefore, a high resolution and a high speed TDC is needed to improve the system performance. Since the maximum distance for the laser rangefinder presented here is targeted to be 60-meters, the TDC should be able to measure time intervals larger than 400ns.

2.2.2. High Voltage Power Supply

To reach the proper gain and responsivity of the APD, a high voltage is used to reverse bias the APD. This high voltage is generated and stabilized using a high voltage DC-DC converter which provides up to 400V output from a 5V input. The high voltage DC-DC converter must provide a low voltage noise and low voltage ripple.

Increasing the voltage output of the DC-DC converter increases the gain of the APD. Therefore, it increases the current output of the APD per optical power. A resistor is connected in series with the APD to limit the current it generates in order to protect the receiving channel from saturation and damage.

2.2.3 Pre- and Post-Amplifiers

A small fraction of the reflected focused on the APD is converted to a voltage signal using a two transimpedance amplifiers. This conversion represents one of the major challenges of the design because bandwidth, gain, and input referred noise are coupled together. Furthermore, to control the transimpedance gain such that the variation of the amount of current generated by the APD does not saturate the system is another challenge.

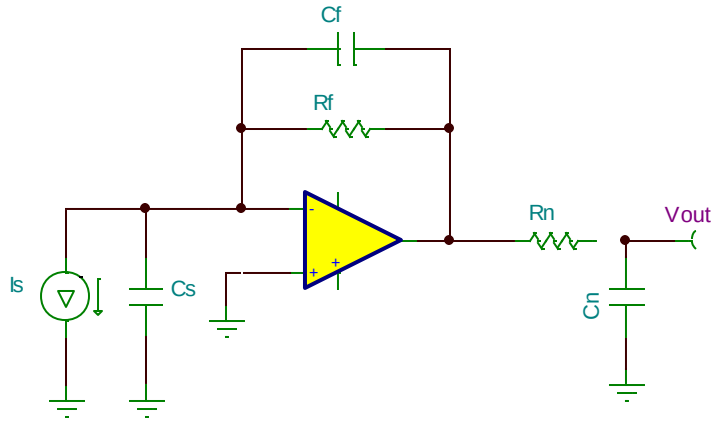

Figure 2.1 Transimpedance amplifier equivalent circuit

The figure above shows the equivalent circuit for a transimpedance amplifier. I_s represents the output current generated by the current source. C_s is the sum of the output capacitance of the current source and the input capacitance of the op amp. R_f is used to convert I_s to a voltage. Therefore, R_f is the gain of the transimpedance amplifier.

At low frequencies, the op amp's inverting input is forced to be at ground potential and I_s must flow through R_f. This combination of effects creates an output voltage of I_s*R_f [17]. At higher frequencies, C_f affects the circuit respond and, together with C_s, has a strong effect on the stability of the amplifier [17]. R_n and C_n are used to reduce the output noise of the amplifier.

2.2.4. Optical Lens

The infrared (IR) light pulses emitted by the PLD are collimated by the transmitter lens. Collimating lens used to reduce to a minimum the divergence of the laser beam such that the laser light does not disperse with distance. An example of an optical collimator is shown in Figure 16.

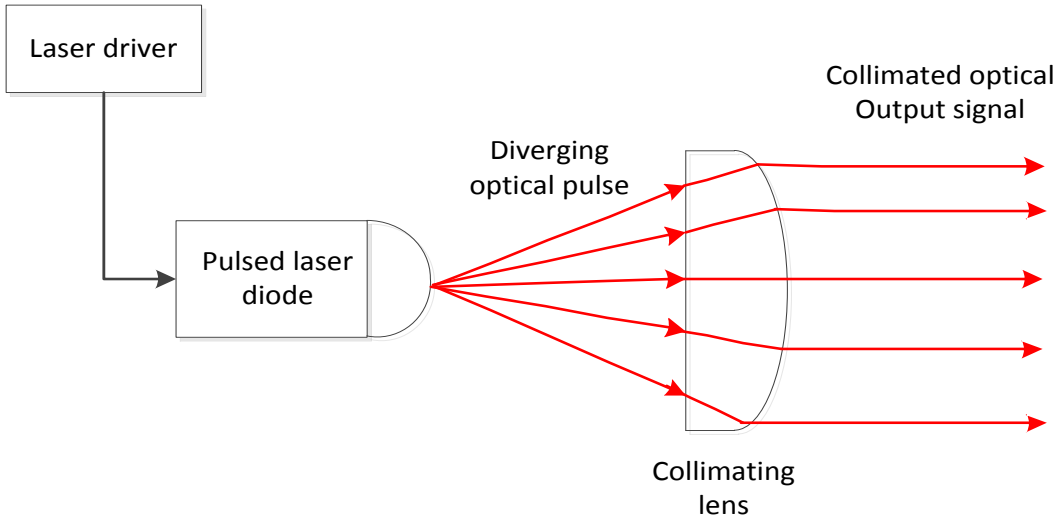

Figure 2.2 Optical collimating lens

The collimating lens used on this project has an antireflective IR coating of 600-1050nm wavelength from ThorLabs, INC.

Figure 2.3 C170TME mounted aspherical lens from Thorlabs, INC

The optical power reflected from the measurement target object is collected, focused and filtered by a plano-convex lens and an optical band-pass filter with an AR coating for 600-1050nm wavelenght. The plano-convex lens is used to focus the collimated reflected laser beam of the target on the APD. The band-pass filter is integrated in the APD and it is used to further block the surrounding light. Using an AR coated lens and a band-pass filter helps to achieve a better signal-to-noise ratio, and minimize the effect of the background light.

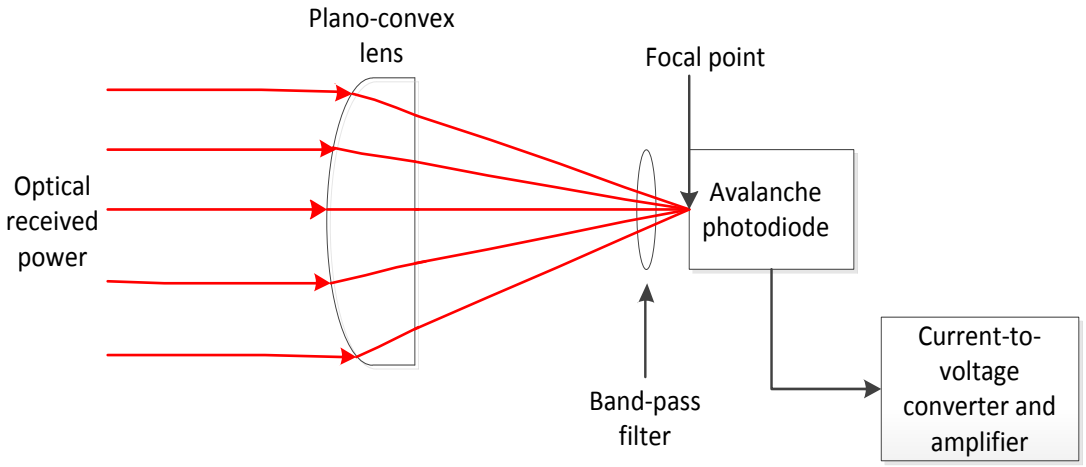

Figure 2.4 Optical receiving lens

3. Design Implementation

This section describes the implementation of each of the subsections discussed in the previous section. The theory, calculations, design considerations and specifications in the previous chapter are used to select the components to implement each subsection. Furthermore, this chapter includes circuit simulation analysis of the implemented subsystems' circuits.

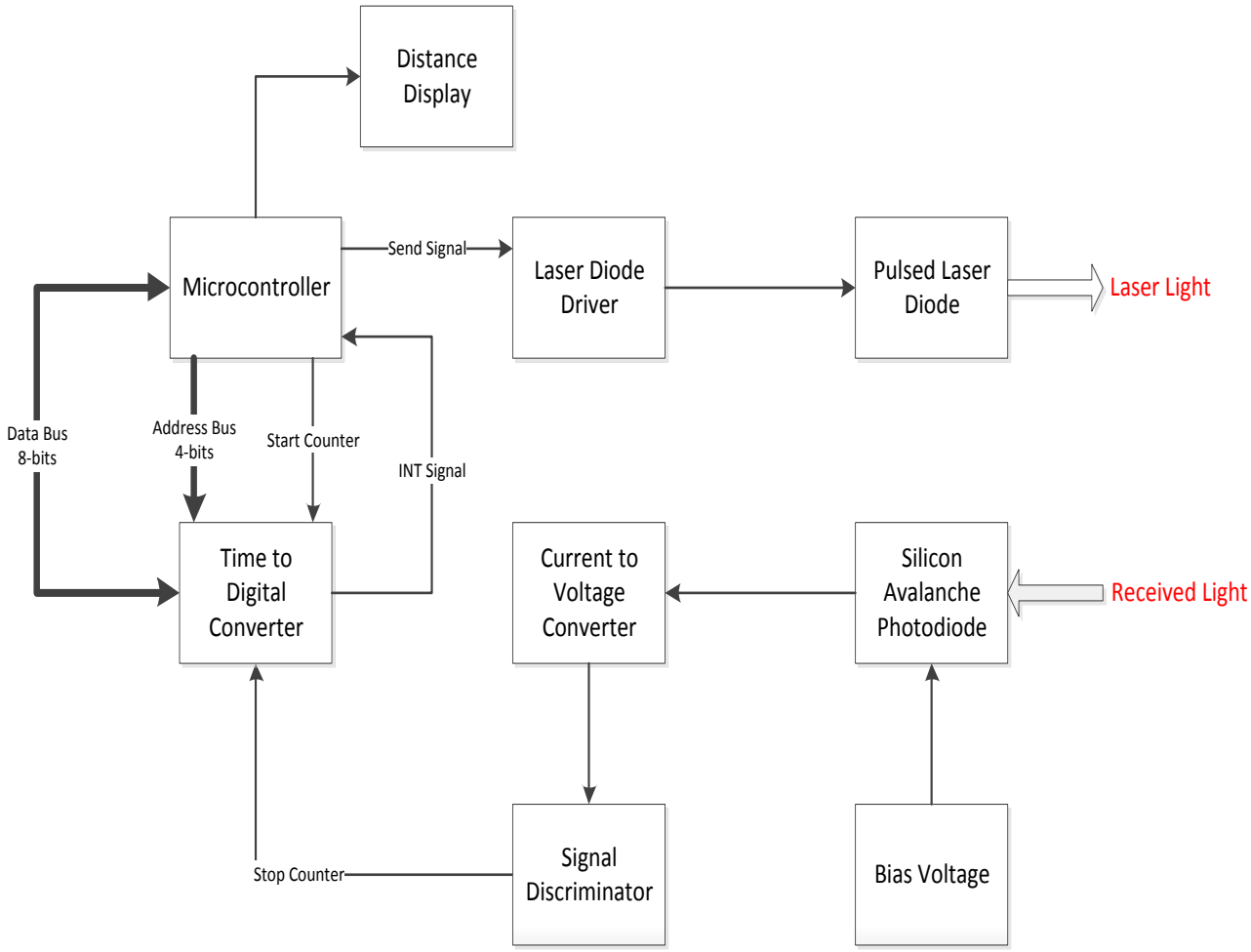

Figure 3.1 Block diagram of the laser rangefinder electronics

3.1. Sending Hardware

This section describes the components and circuits used in the implementation of the sending channel of the rangefinder. This channel is designed such that short and powerful light pulse are generated and sent toward a target measurement object. Also, this section describes the system controller and its speed.

3.1.1. Microcontroller

The microprocessor used for this design was the ATMega128 from AVR. The ATmega128 is a low-power CMOS 8-bit microcontroller based on the AVR enhanced RISC architecture. By executing powerful instructions in a single clock cycle, the ATmega128 achieves throughputs approaching 1 MIPS per MHz to optimize power consumption versus processing speed[1]. The ATmega128 clock speed is set to 16MHz.

[1] ATMega128 Product datasheet

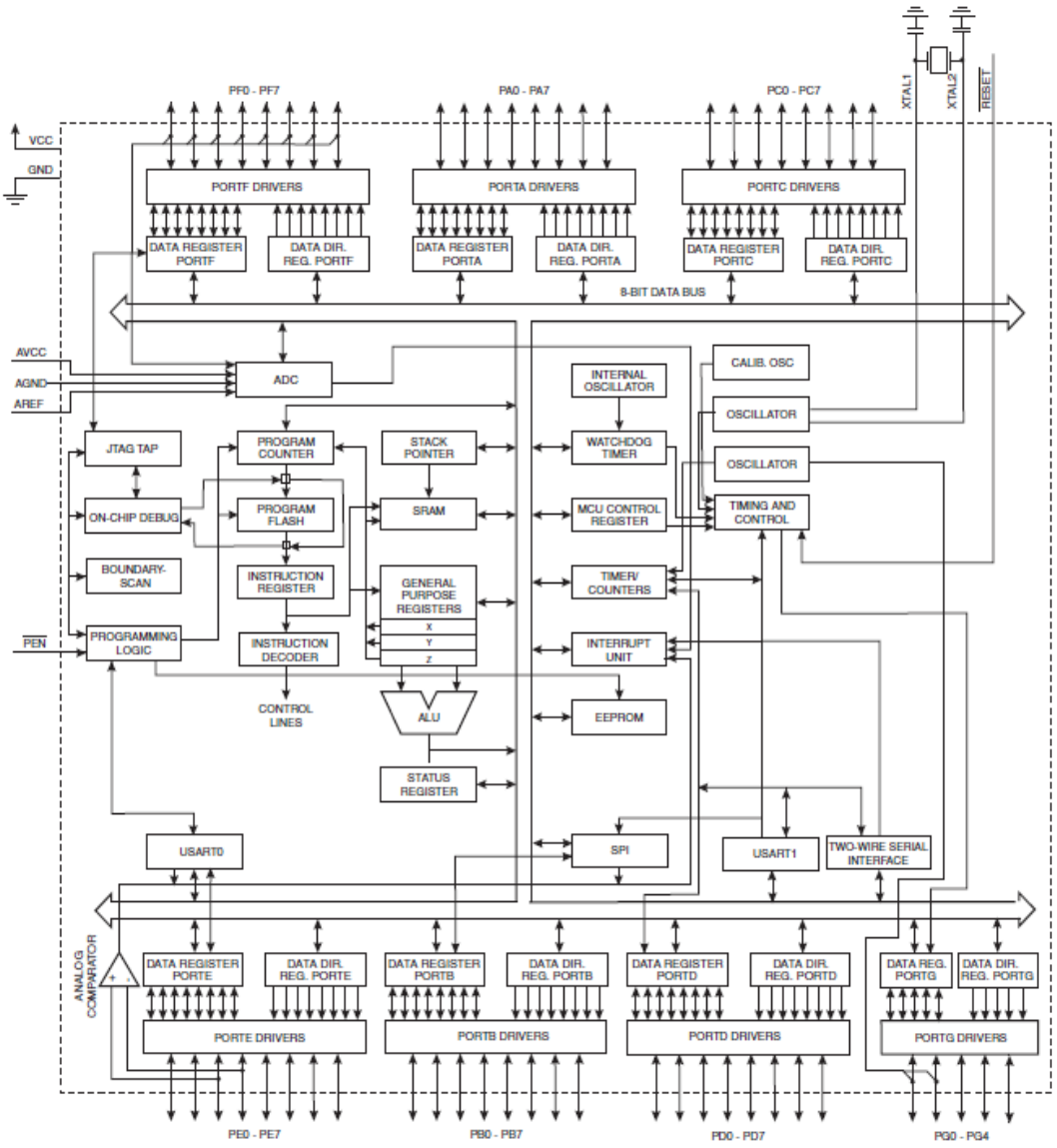

Figure 3.2 Block diagram of the ATMega128

A 125ns pulse is generated using PORTD of the ATMega128. This pulse starts the counter in the TDC-GP1, and to send the laser signal. Also, the ATMega128 is used to read the time calculated by the TDC-GP1 and calculate the distance. The calculated information is sent to the host computer through USART interface.

3.1.2. Pulsed Laser Diode and Driver Circuit

The light emitting circuit implemented in this research outputs a short and powerful pulse of laser beam toward a measurement target object. It is composed of a 905 nm wavelength PLD (905D1S1.5 from Laser Components, INC.); a fast switching MOSFET (IRF840) to turn on/off the PLD; and a MOSFET driver (EL7104 from Intersil Corporation). Figure 7 shows the implemented circuit to drive the 905D1S1.5 PLD.

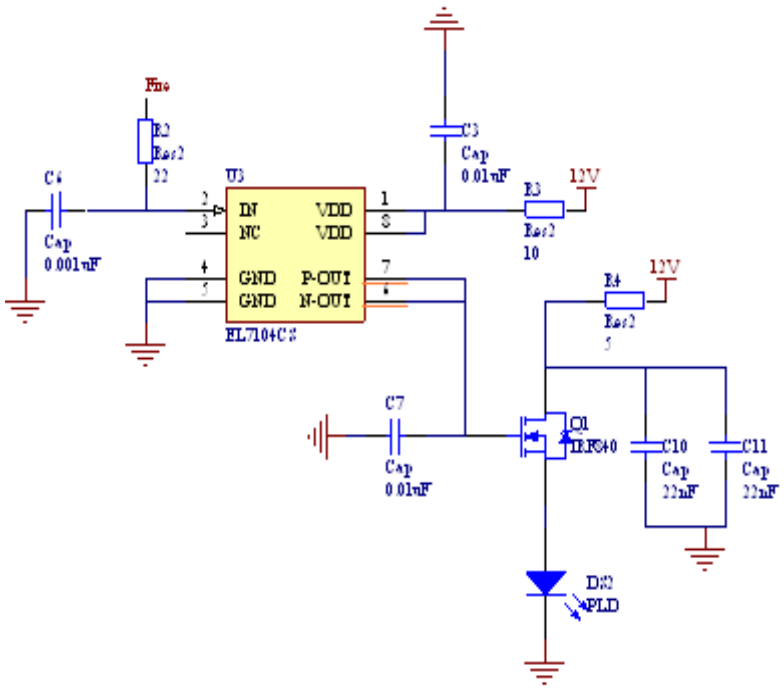

Figure 3.3 Pulsed laser diode driver

The circuit for the EL7104 was implemented using [2]. A 125 ns pulsed is sent from the microcontroller to the EL7104 driver that increases the TTL level voltage to 12V with a propagation delay of 18ns. This allows the laser to turn-on for the time mentioned. The input current to the PLD is limited to 2.4A by using a 12V input and 5Ω resistor.

3.2. Receiver Hardware

The light receiver circuit is composed of the SARF500F2 905nm wavelength avalanche photodiode from Laser Components, INC., for photo-electrically converting the reflected light; a high voltage DC-DC converter to bias the SAR500F2; a two-stage amplifier to convert to voltage and amplify the small current generated by the SAR500F2; and TDC to measure the time interval between the sent and received signals. The SARF500F2 operates in avalanche breakdown mode and creates a high gain junction. In order to operate the SARF500F2 in the breakdown mode, it must be reverse biased with a minimum of 300V.

3.2.1. Time to Digital Converter

As mentioned in the previous chapter, a fast-speed TDC is need to measure the time-of-flight of the pulsed light. This system uses the TDC-GP1 to measure the time-of-flight. The TDC-GP1 can be utilized either 1-channel with a high resolution mode of 125ps which is equivalent to 19mm distance or 2-channels with a 250ps resolution with is equivalent to 38mm distance The TDC-GP1 measures the time different between a START and STOP input signals. The TDC-GP1 transforms time intervals calculated into digital values with high precision. When the time interval is calculated by the TDC-GP1, it generates an interrupt signal to start reading the time result from its registers.

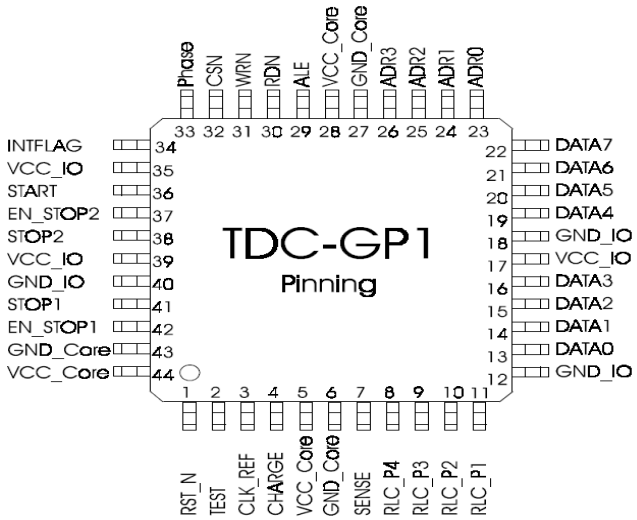

Figure 3.4 TDC-GP1 pinout

3.2.1.1. Key Features

Some of the key features of the TDC-GP1 are:

- Allows double pulse resolution of approximately 15 ns.
- Two Measurement ranges : 3 ns to 7.6 µs and 60 ns to 200 ms.
- Up to 8-events on both channels that can be measured against one another arbitrarily, no minimum time difference.
- Up to 4 calibrated or 8 uncalibrated measurement values can be stored internally.
- Calibration and control clocks from 500 kHz up to 35 MHz.
- Variable edge sensitivity of the measuring inputs.
- Small 44-TQFP package.
- Extremely low power consumption.

3.2.1.2. Microprocessor Interface

The TDC-GP1 provides a standard 8-bit microcontroller parallel interface. The TDC-GP1 has seven 8-bits write only registers, four 8-bits value control registers, 8 only read results registers for the measurement result. It has a 4-bits address bus and an 8-bits data bus. The time calculation values and the status of the TDC-GP1 can be read out via the following signals: ALE, RDN, WRN and CSN which correspond to pins 29-31 as seen on the TDC-GP1 pinout.

3.2.1.3. Measurement Range Mode

The TDC-GP1 is operate using measurement range mode 1 which offers a 2 channel TDC with common start, and allows 4-hits per channel with a resolution of 125 ps. This mode is used because of its higher resolution when compare to mode 2. Also, it allows shorter distance measurements.

The TDC-GP1 is controlled and initialized by addressing the values on the control registers. The TDC-GP1 is initialized to work on measurement mode 1 with high resolution by writing the following values to the control registers:

- REG0= 0x48 – Measurement range 1, Auto_cal + Calibrate
- REG1= 0x4D – High resolution, precision adjust mode 4D

- REG2= 0x01 – Set Hit1 on Channel 1 – Start
- REG4= 0x80 – Set calibrate clock to run at 20MHz/16= 1.25MHz
- REG6= 0x02 – Set the ALU speed to medium
- REG7= 0x01 – Enable one stop on Channel 1

3.2.2. High Voltage Supply

Different circuit were simulated and tested to provide high voltage output from a low voltage input with a low voltage noise. The circuit from [9] on Figure 3.5 was simulated using LTSpice IV from Linear Technology, INC. and built to test its capabilities of providing a low noise bias voltage for the APD.

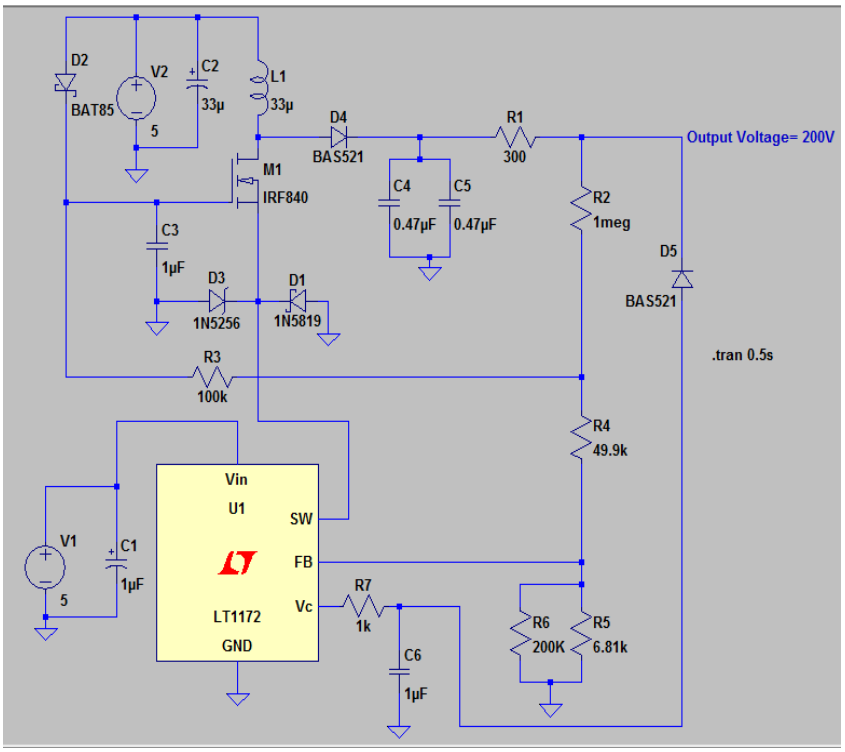

Figure 3.5 5V to 200V Output converter for APD bias

As explained on [9], the circuit is a basic inductor flyback boost regulator with a major important deviation. The IRF840 MOSFET, a high voltage device, has been interposed between the LT1172 switching regulator and the inductor. This permits the regulator to control the IRF840's high voltage switching without undergoing high voltage stress. The IRF840, operating as a "cascode" with the LT1172's internal switch, withstands L1's high voltage flyback. For more information, please refer to [9, page 20]. The gain of the SARF500F2 APD was too small with a 200V bias. The current generate by the APD was too small to be detected by the amplification circuit. Furthermore, a high voltage ripple was generated by the circuit causing the receiver channel to read false STOP signals.

A device or circuit that provides a voltage output up to 350V was required such that the gain of the APD was at least 100. A micro-size high voltage DC-DC converter as the 0.4US5-P0.1 from Ultravolt, INC is used. This DC-DC converter offers a low-voltage ripple (<20mV peak to peak), small package size, lightweight (around 13g), and low noise due to its metal shielding. Figure 3.6 shows the circuit implemented using the 0.4US5-P0.1 DC-DC converter.

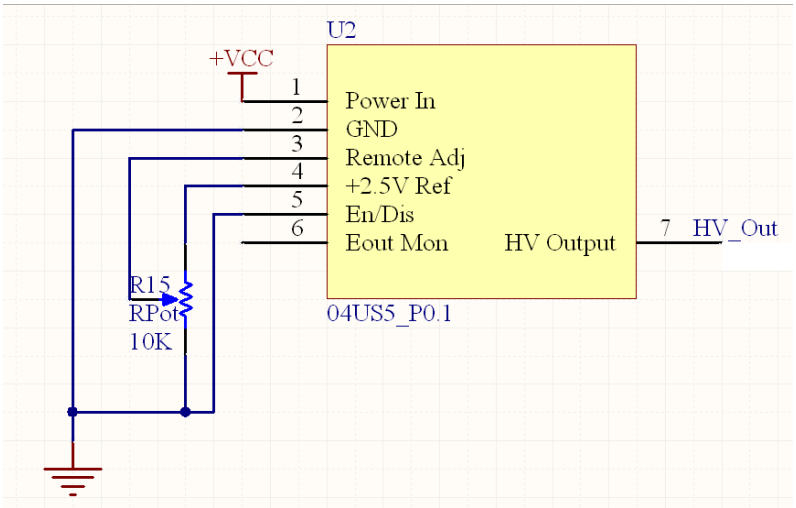

Figure 3.6 High voltage DC-DC converter

The output voltage of the 0.4US5-P0.1 is adjusted by changing the voltage applied to its remote adjust input (pin 3) by changing the value of R15. The output voltage of the 0.4US5-P0.1 is set to 350V. This way, the gain of the SARF500F2 is 100. The only drawback of this device is that the maximum current output is 250µA. Therefore, the maximum current that could be generated by the APD is also 250µA.

3.2.3. Current to Voltage Converter and Amplifier

The op amps tested and used in this design are the OPA656 which has a gain bandwidth product (GBP) of 230 MHz with a 7nV/ √Hz input noise, the OPA657 which GPB is 1.65GHz with a 4.8nV/ √Hz input voltage noise, and the OPA846 which has a 1.75GHz GBP with a 1.2nV/ √Hz input voltage noise. All these devices are from Texas Instruments, INC. The transimpedance amplifiers circuits using these components were simulated using TINA Simulator from Texas Instrument.

Since the maximum current supply by the DC-DC converter is around 250µA, the maximum current generated by the APD is around 250µA. Knowing the expected maximum current, the gain of the transimpedance amplifier can be chosen for both pre- and post-amplifiers. The value of R_f was chosen to be 10kΩ such that the maximum voltage output at the pre-amplifier is around 2.5V. The output capacitance of the APD with a 350V bias is around 1pF according to figure 5 in the data sheet for the SARF500F2 [10].

To achieve a maximally flat 2nd-order Butterworth frequency response, the feedback pole should be set to [11], [12]:

$$\frac{1}{(2\pi RfCf)} = \sqrt{\frac{GBP}{(4\pi RfCs)}} \qquad (1)$$

Using the values of C_s for the different op amps, targeting a 10kΩ transimpedance gain and using their GBP of each op amp, the following feedback poles are obtained:

Table 1 Transimpedance amplifier feedback pole values

Device	GBP (MHz)	Feedback pole (MHz)
OPA656	230	42.782
OPA657	1650	114.587
OPA846	1750	118.009

Using Equation 1 and the calculated values for the feedback poles, the following values for the feedback capacitor, C_f, of each op amp is obtained:

Table 2 Transimpedance amplifier feedback capacitor values

Device	Feedback capacitor (pF)
OPA656	0.37202
OPA657	0.1389
OPA846	0.1349

The maximum bandwidth will be achieved for a Butterworth response with Q= 0.707 [11]. To determine the GBP requirements for the transimpedance amplifiers, equation 12 of [11] was used:

$$GBP = 2\pi \bullet F^2_{-3dB} \bullet R_f C_s \qquad (2)$$

This gives an approximate -3dB bandwidth set by:

$$F_{-3dB} = \sqrt{\frac{GBP}{2\pi Rf(Cs+Cf)}} \qquad (3)$$

Knowing the values for R_f, C_s, C_f and the GBPs of the op amps, the transimpedance bandwidth can be calculated using equation 3.

Table 3 Transimpedance amplifier -3dB computed bandwidth values

Device	Input Capacitance (pF)	Source Capacitance (pF)	Max Bandwidth (MHz)
OPA656	3.5	4.5	27.6155
OPA657	5.2	6.2	64.5627
OPA846	3.8	4.8	75.3930

3.2.3.1 Noise Analysis

The dominant noise sources of the receiver channel are the thermal noise generated by R_F and the noise generated by the input of the transimpedance preamplifier. This noise can be reduced using high R_F values which imply increasing the gain of the preamplifier. The transimpedance amplifier circuits using the OPA656, OPA657 and OPA846 op amps were designed and tested using TINA Simulator. The noise parameters for the op amps are calculated using [17]. The following values are obtained for the **OPA656**:

- Low –frequency noise gain (G_{N1})= 1 V/V
- High-frequency noise gain (G_{N2})= 1 + C_S/C_F= 10 V/V
- Noise gain's zero (f_{NZ})= $1/(2\pi R_F (C_F+ C_S))$= 3.32MHz
- Noise gain's pole (f_{NP})= $1/(2\pi R_F C_F)$= 31.831MHz

The following values are calculated for the **OPA657**:

- G_{N1}= 1 V/V
- G_{N2}= 1 + C_S/C_F= 21.7 V/V
- f_{NZ}= $1/(2\pi R_F (C_F+ C_S))$= 3.25MHz
- f_{NP}= $1/(2\pi R_F C_F)$= 53.1MHz

The values for the OPA846 are very similar to the values of the OPA657 because they have similar GBPs, but the OPA846 introduces a higher noise frequency. This is in agreement with [16, page 7] which shows that for transimpedance gains greater than 2kΩ, a field-effect transistor (FET) such as the OPA656/657 will have a lowest input-referred noise when compare to the OPA846 bipolar amplifier. Therefore, the OPA846 was discarded from the op amp choices.

The value of the feedback capacitor was increase for the designs of the transimpedance amplifiers using the FET amplifiers. C_F= 3pF and C_F= 2pF were used for the OPA657 and OPA656 respectably. The system still stable and G_{N2} is reduced to 2.94V/V for the OPA657 and 3.05V/V for the OPA656.

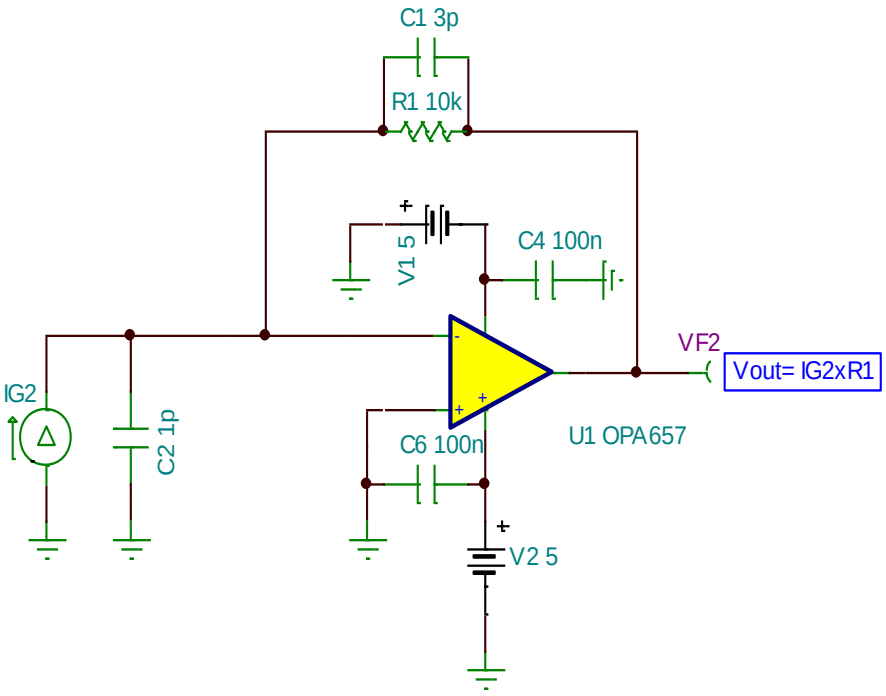

Figure 3.7 Transimpedance amplifier circuit using the OPA657

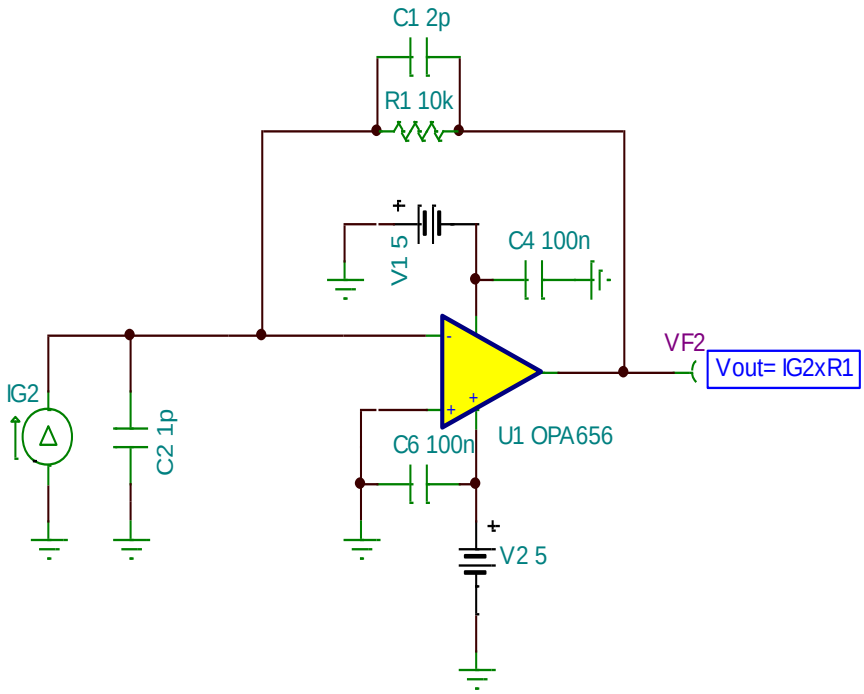

Figure 3.8 Transimpedance amplifier circuit using the OPA656

The following graphs show the simulation results of the above circuits:

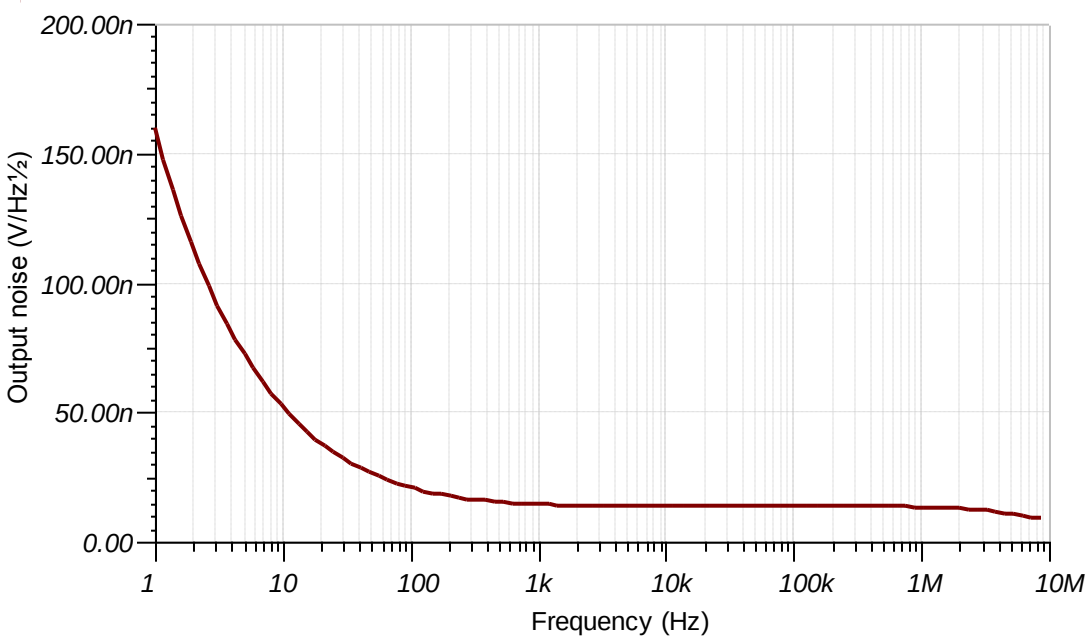

Figure 3.9 Output noise of the transimpedance amplifier using the OPA657

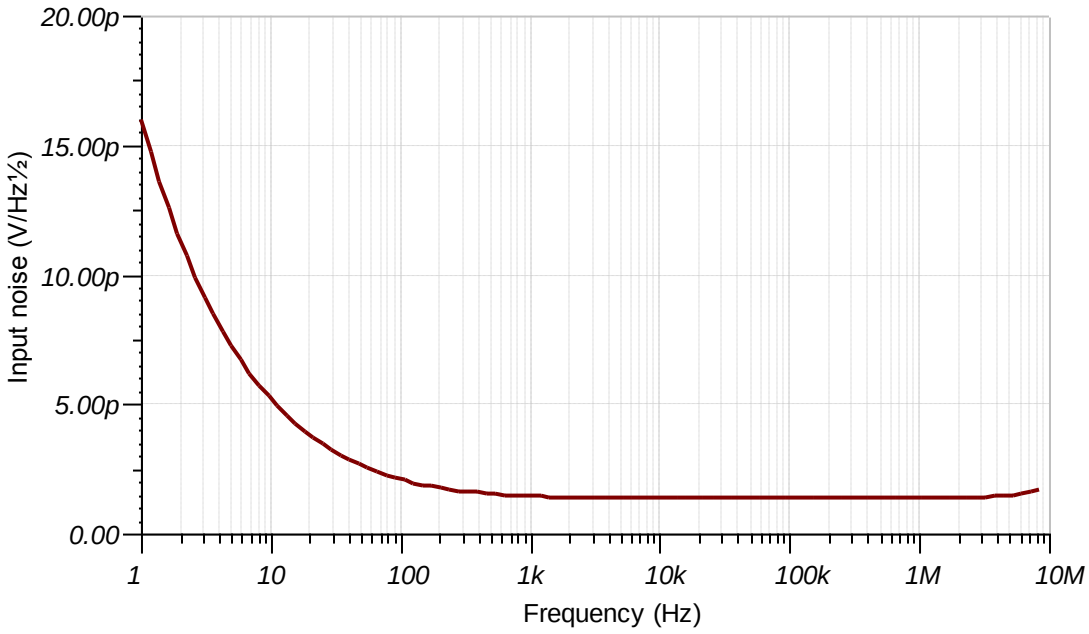

Figure 3.10 Input noise of the transimpedance amplifier using the OPA657

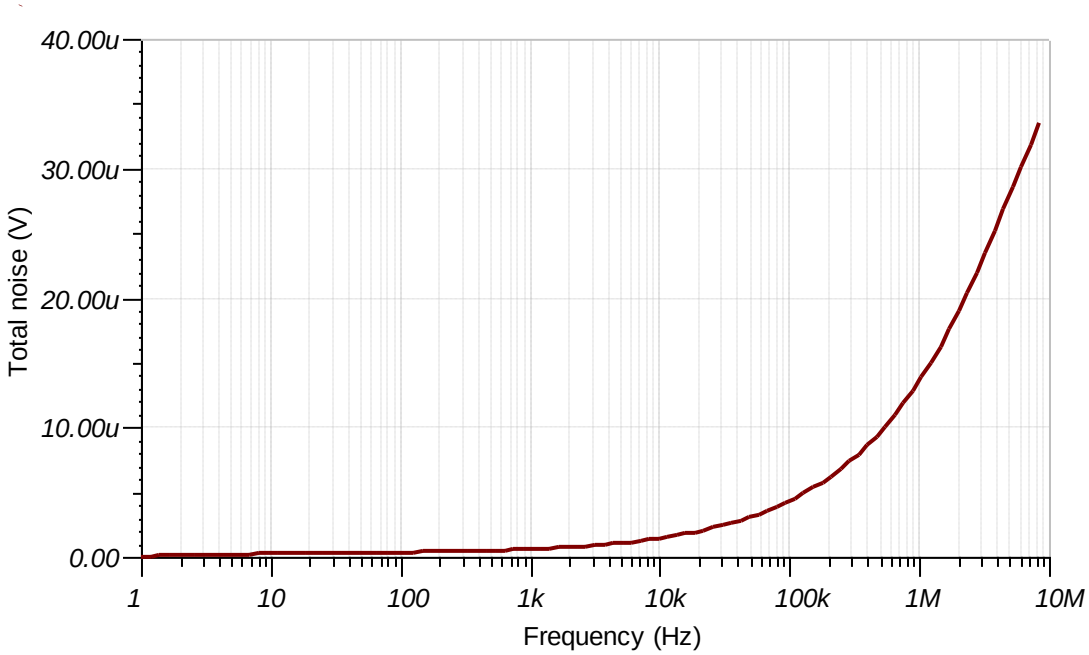

Figure 3.11 Total noise of the transimpedance amplifier using the OPA657

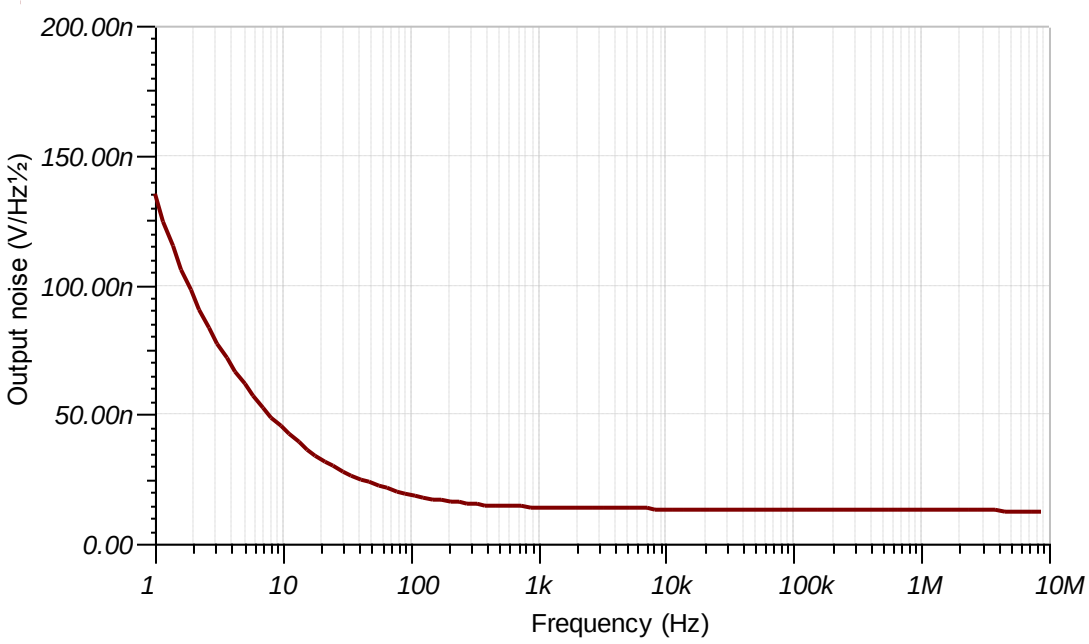

Figure 3.12 Output noise of the transimpedance amplifier using the OPA656

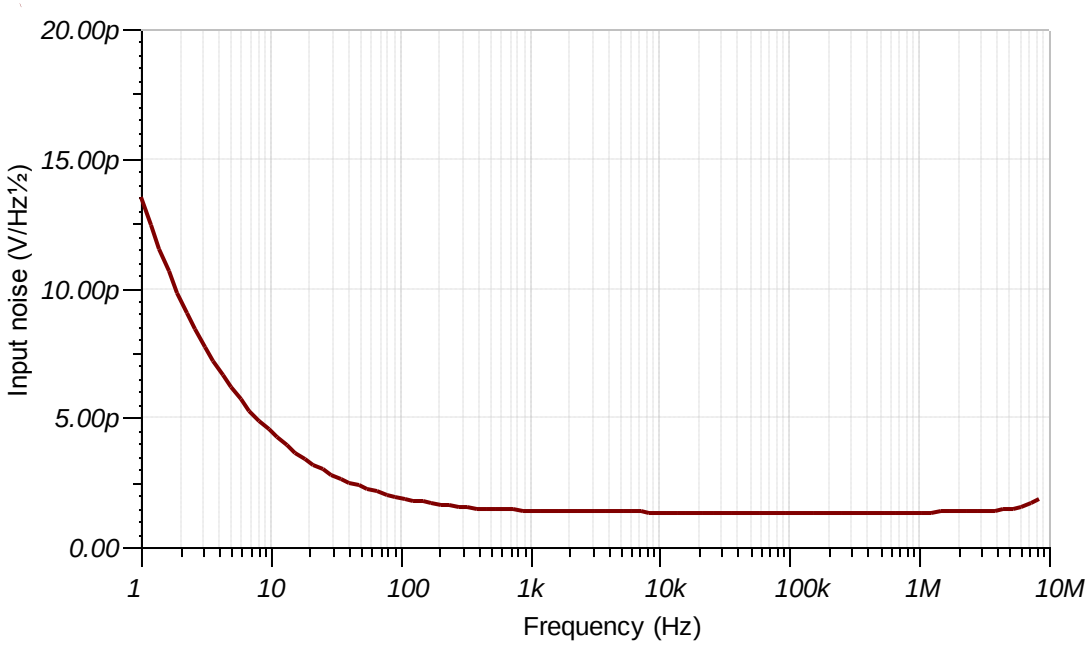

Figure 3.13 Input noise of the transimpedance amplifier using the OPA656

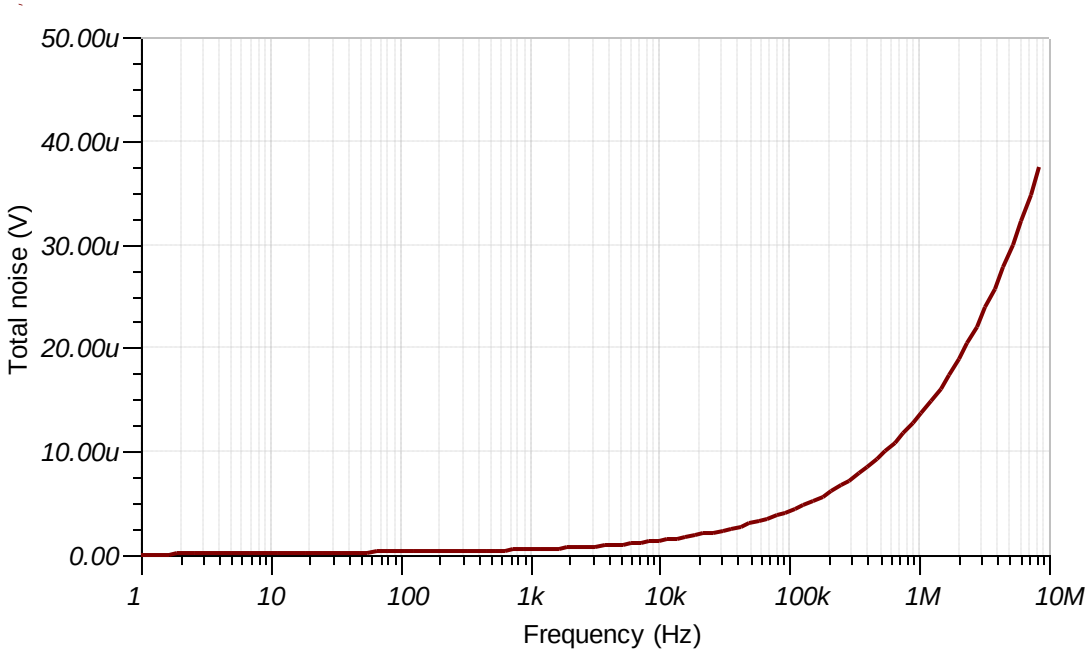

Figure 3.14 Total noise of the transimpedance amplifier using the OPA656

For this design, the OPA656 was chosen because of its lower input and output noise as can be seen in the figures above. To further reduce the output noise, a low-pass filter is connected at its output. The cut-off frequency (f_C) of this filter needs to be below the f_{NZ}= 2.45MHz. Since each laser pulse is 125ns with a 125µs delay, the f_C for the low-

pass filter must be above 8kHz. The f_C of the filter is set to 10.61KHz using R_N= 1.5kΩ and C_N= 10nF. The following total noise is generated at the transimpedance circuit:

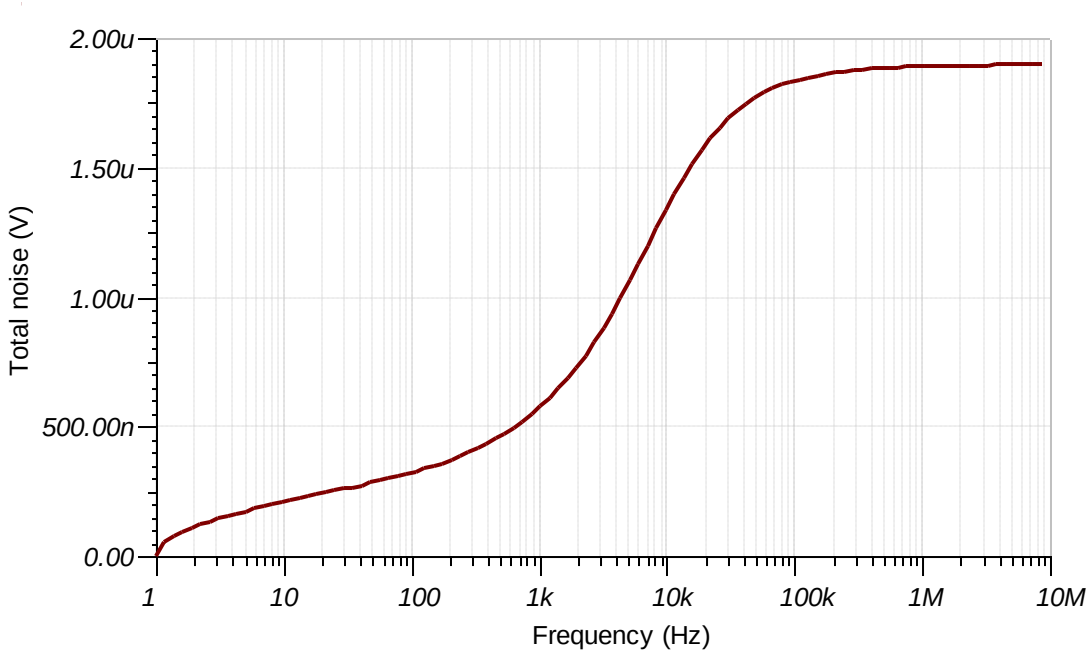

Figure 3.15 OPA656 filtered noise signal

A post-amplifier is used to amplify the voltage pulse further. The post-amplifier is also designed using the OPA656. Its bandwidth is designed to be sufficiently wide that it does not degrade the bandwidth of the channel. Figure 3.16 depicts the receiver channel's circuit implemented on this work:

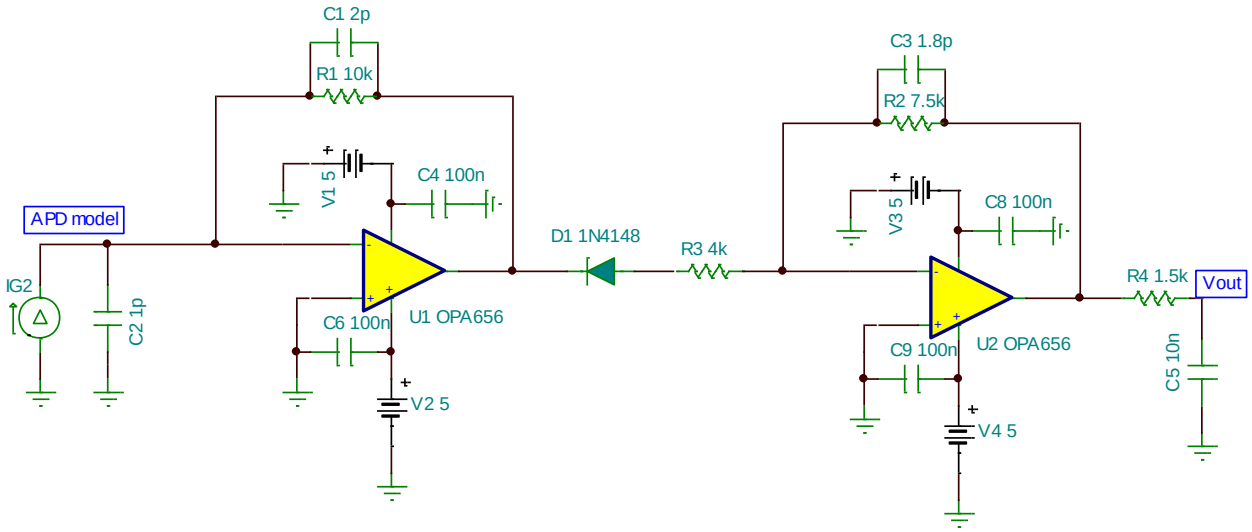

Figure 3.16 Receiver channel amplifying circuit

This circuit design was simulated using TINA Simulator. A fast silicon diode (1N4148) is used to reduce the noise output of the first-stage transimpedance amplifier. The simulation results are shown in the figures below.

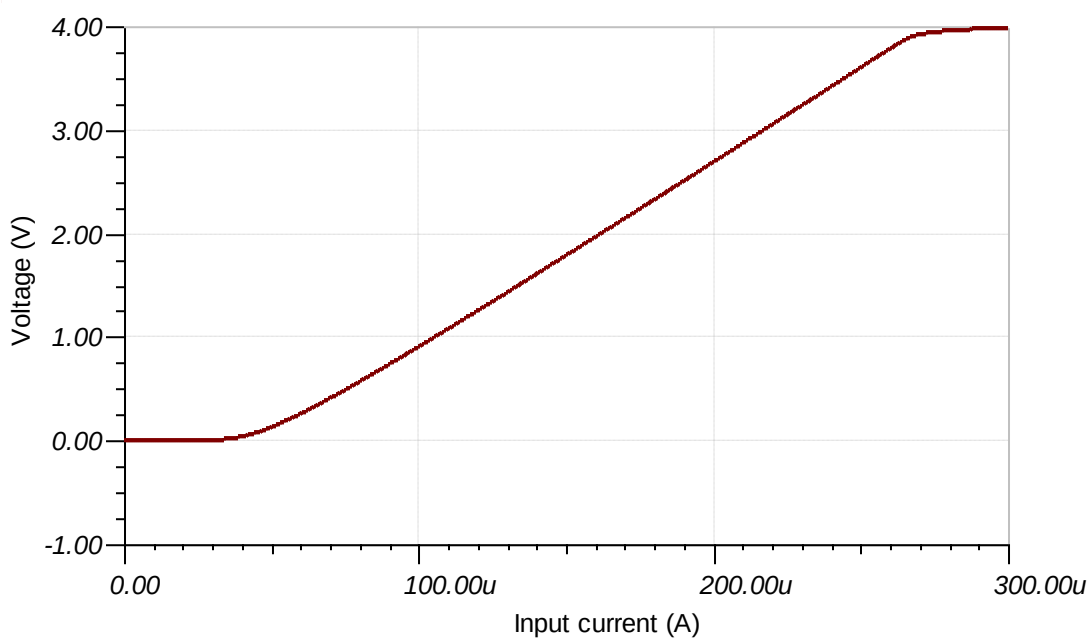

Figure 3.17 DC transfer characteristic of the amplifying circuit

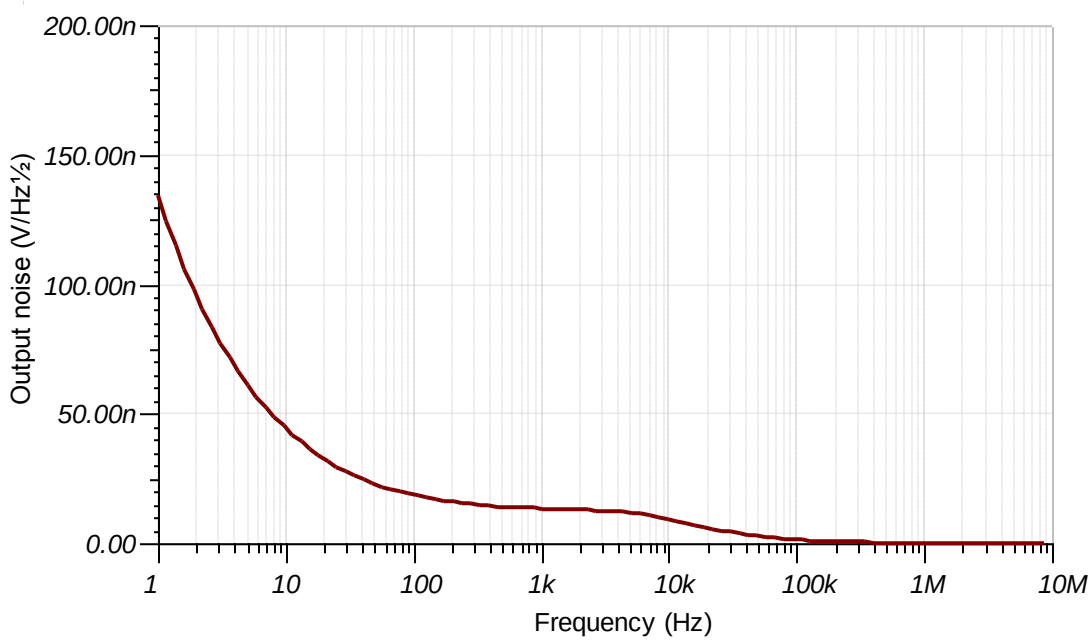

Figure 3.18 Output noise of the amplifying circuit

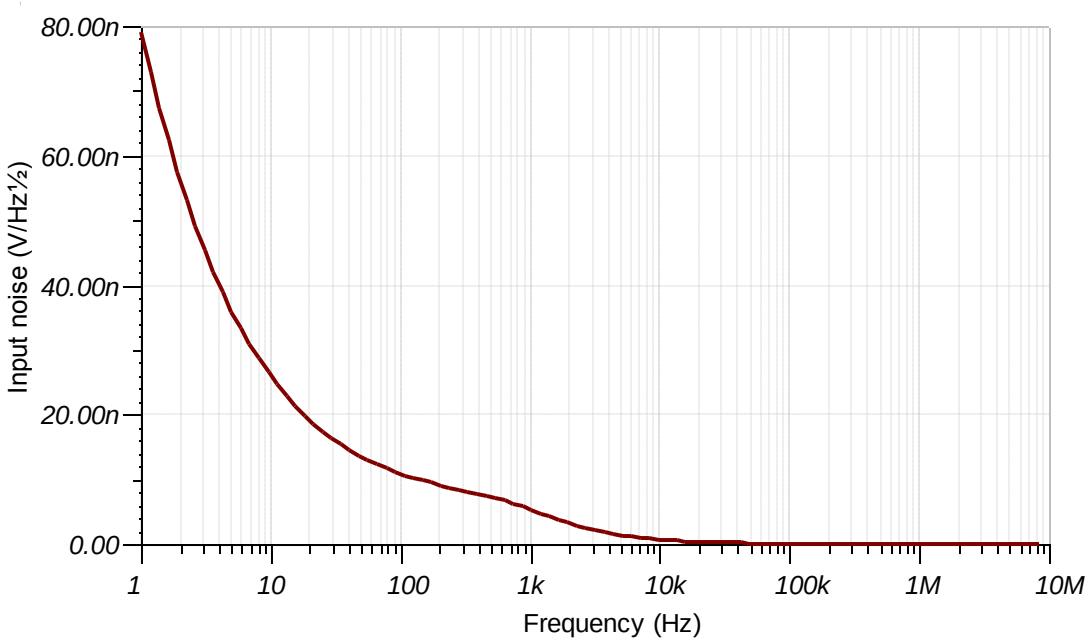

Figure 3.19 Input noise of the amplifying circuit

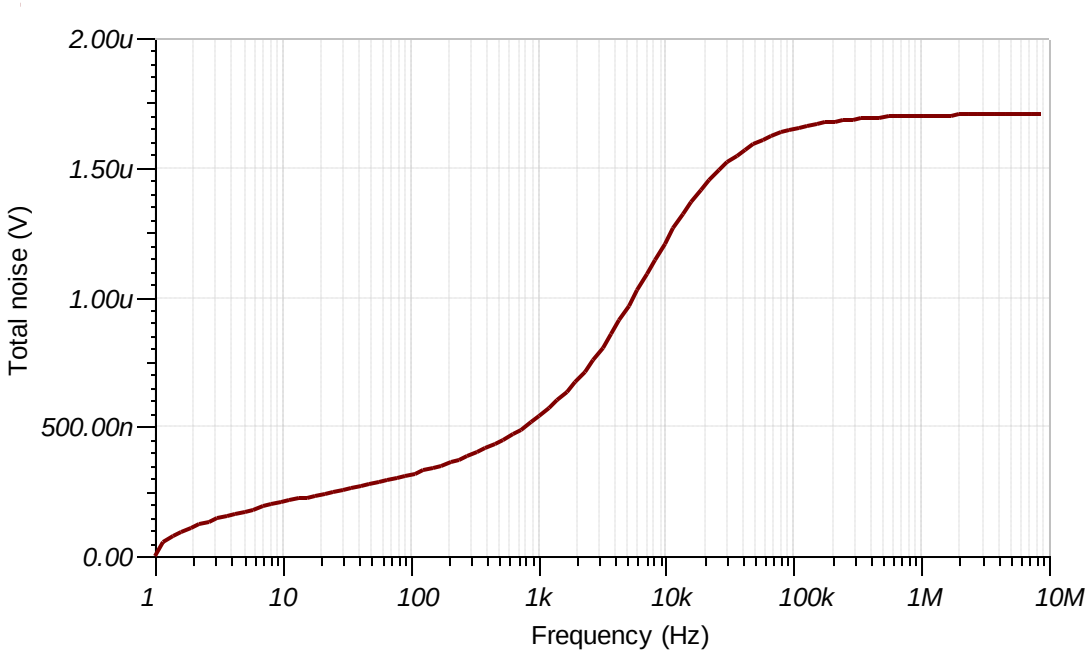

Figure 3.20 Total noise generated by the amplifying circuit

3.2.4. Signal Discriminator

This section describes the signal discriminator implemented to differentiate between the received signal and the noise generate at the receiver. In this implementation, a leading

edge discriminator is designed and tested using two types of ultra-fast and high precision comparators: LT1016 and LT1394 both from Linear Technology Corporation.

The LT1016 is a 10ns propagation delay comparator that interfaces directly to TTL/CMOS logic while operating off either ±5V or single 5V supplies. Figure 3.21 shows the circuit used to test the respond time of the LT1016.

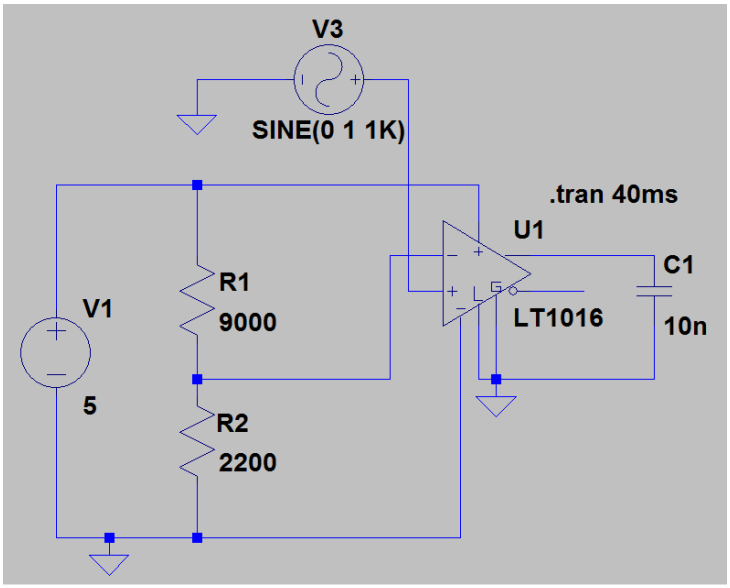

Figure 3.21 LT1016 voltage comparator

The circuit above was built and tested. The minimum voltage reference for this comparator is 1.2V when using a single supply as it is mentioned in the LT1016 datasheet. A voltage reference of 1.2V is too high when compared to 50mV noise signal at the input of the comparator.

A second circuit was tested using the LT1394 which is pin compatible with the LT1016. The LT1394 offers a 7ns propagation delay which helps to reduce the systematic delay of the receiver channel. The LT1394 has an input voltage range from 0 to 3.5V when using a single 5V supply voltage. This device is used in the implementation of the receiver channel with a voltage reference of 80mV (30mV above the measure signal noise).

3.3. PCB Design

After the circuits for the sender and receiver channels were tested on a breadboard, the PBC was designed using Protel DXP 2004. Designing a PCB which reduces the propagation of the received signal helps to reduce the systematic error of the system. The size of the board is 3-inches by 3-inches. A smallest size could not be achieved because of the difficulties of soldering micro-size components by hand. The figures bellow shows PCB designed for the laser rangefinder implemented in this research.

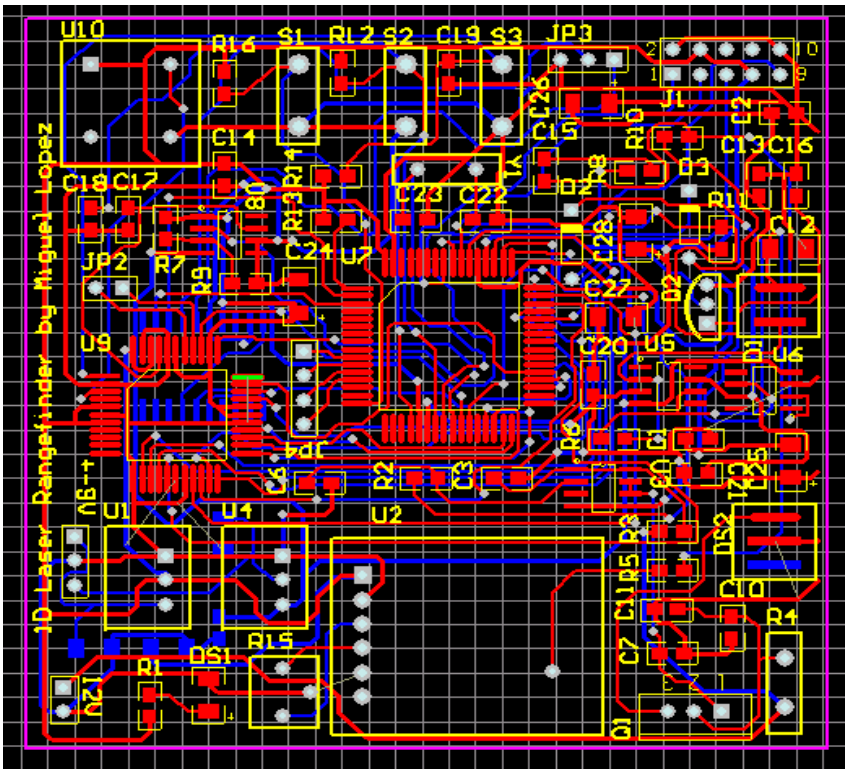

Figure 3.22 PCB of laser rangefinder

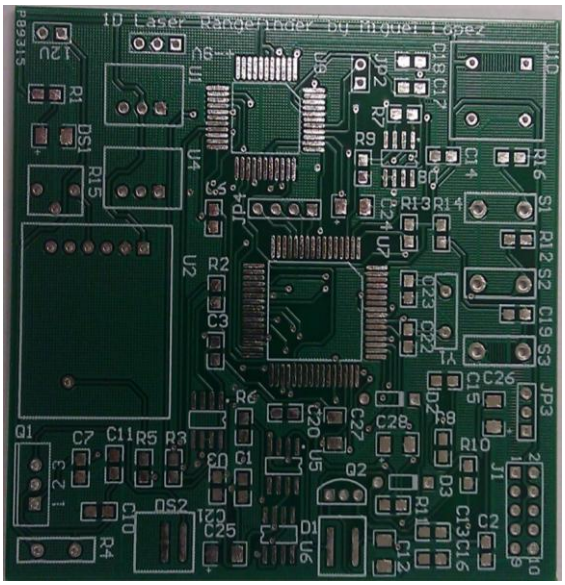

Figure 3.23 Unpopulated rangefinder board

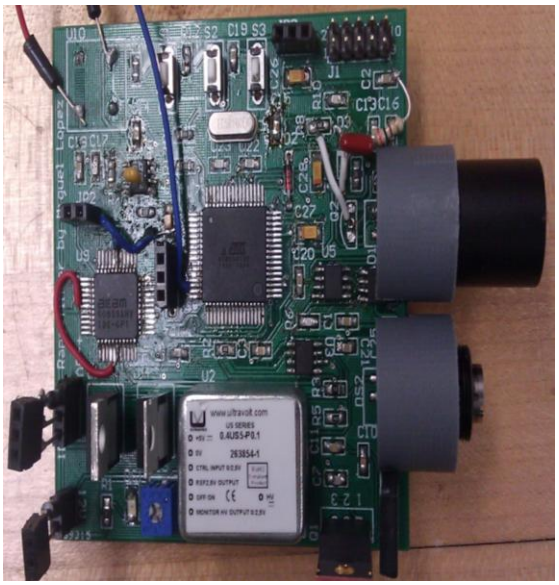

Figure 3.24 Populated rangefinder board

4. System Testing

This chapter describes the measured results when testing the designed laser rangefinder. First, the interface of the microcontroller with the TDC-GP1 was tested to determine how accurate the time measured is. Later, the circuits for the sending and receiving channels were implemented and tested shielding the following results.

4.1. Microcontroller –TDCGP1 Interface

This section shows the time measurement obtained when interfacing the ATMega128 with the TDC-GP1. As previously mentioned, the ATMega128 is running at 16MHz and the reference clock for the TDC-GP1 is set to 1.25MHz. Figure 4.1 shows how the ATMega128 is connected with the TDC-GP1.

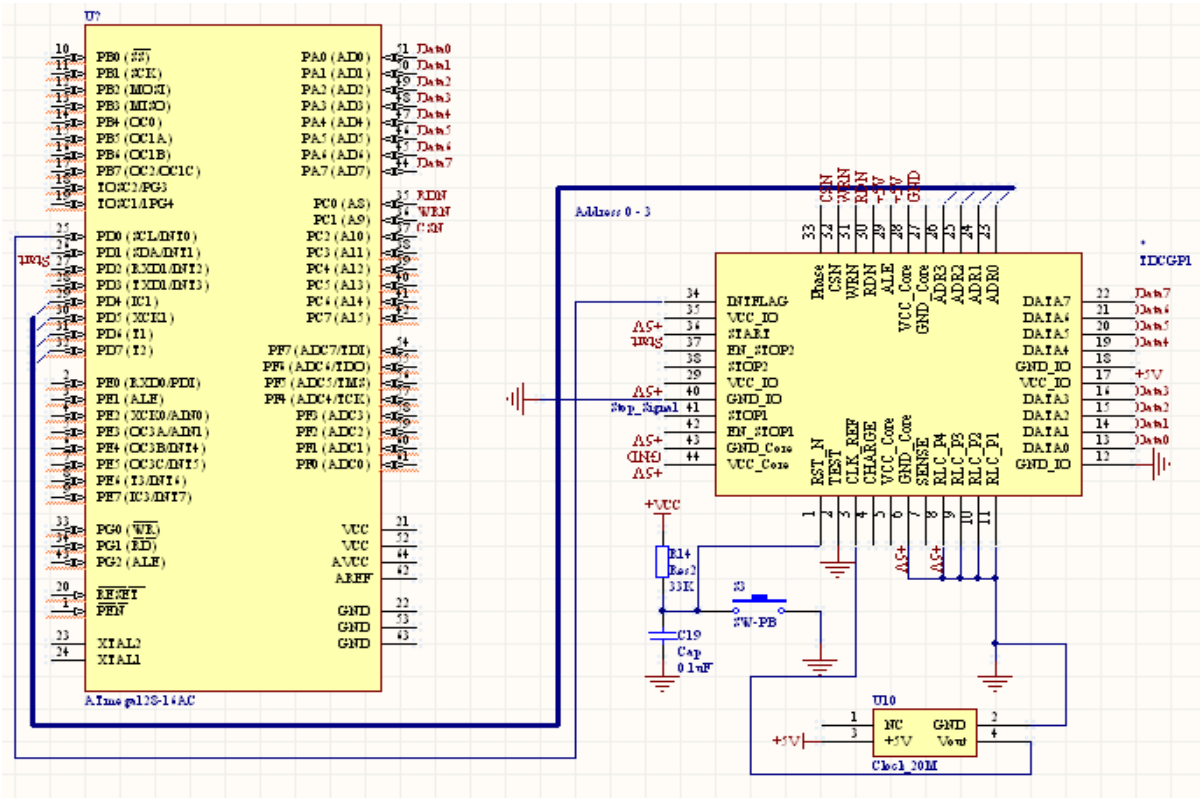

Figure 4.1 ATMega128 and TDC-GP1 interface

PORTA is used to initiate the GP1, set its parameters and read the time information. The address bus of the GP1 is connected to pins 4, 5, 6, and 7 of PORTD. The INT signal of the GP1 is connected to INT0 of the ATMega128. The RDN, WRN and CSN pins of the GP1 are connected to pins 0, 1 and 2 of PORTC respectively.

The table bellow shows the time measured by the GP1 after sending different delayed signals from the microcontroller. The left column shows the time measured using a 100MHz oscilloscope and the right column the time measured by the GP1.

Table 4 TDC-GP1 testing measurements

Time observed in oscilloscope	Time Measured by TDC-GP1
489 ns	487.1429 ns
610 ns	608.4286 ns
740 ns	731.8571 ns

860 ns	859.7143 ns
984 ns	984.8571 ns
1106 ns	1106.25 ns
1228 ns	1229.286 ns
1352 ns	1352.5 ns
1476 ns	1475.571 ns
1600 ns	1598.857 ns

As can be seen from Table 4, the different between the time measured by the oscilloscope and the time measured by the GP1 is less than 2ns for the different delayed signals except for row-four where the different is almost 9ns. This is caused by an error during measurement and it is not taken into considerations because of the agreement of all the others measured values.

4.2. Distance Measurement

The implemented laser rangefinder's capability to measure range is tested. The time measured for distances up to 5-meters is presented. The time measured for the implemented system is expected to increase linearly with distance. The table bellow shows the time measured at a reference distance with the corresponding standard deviation of the measurements.

Table 5 Time of flight measured

Distance (m)	Time_Avg (ns)	STDDEV(ns)
0.3	3.8776	0.194999796
0.6	12.08926	0.070016033
1	20.43533	0.224011947
1.3	24.68651	0.213276478
1.6	28.32517	0.254478447
2	37.86404	0.285151948
2.3	44.22642	0.270473239
2.6	49.75942	0.267926581

3.01	55.30008	0.242158148
3.3	62.67117	0.58272521
3.97	72.7074	0.492283922

The reference distance was measured using a measurement tape. At each distance, more than 1000 time measurements are taken and it average is shown on the second column of the table. Figures 29 and 30 show the graphs of the measurement obtained.

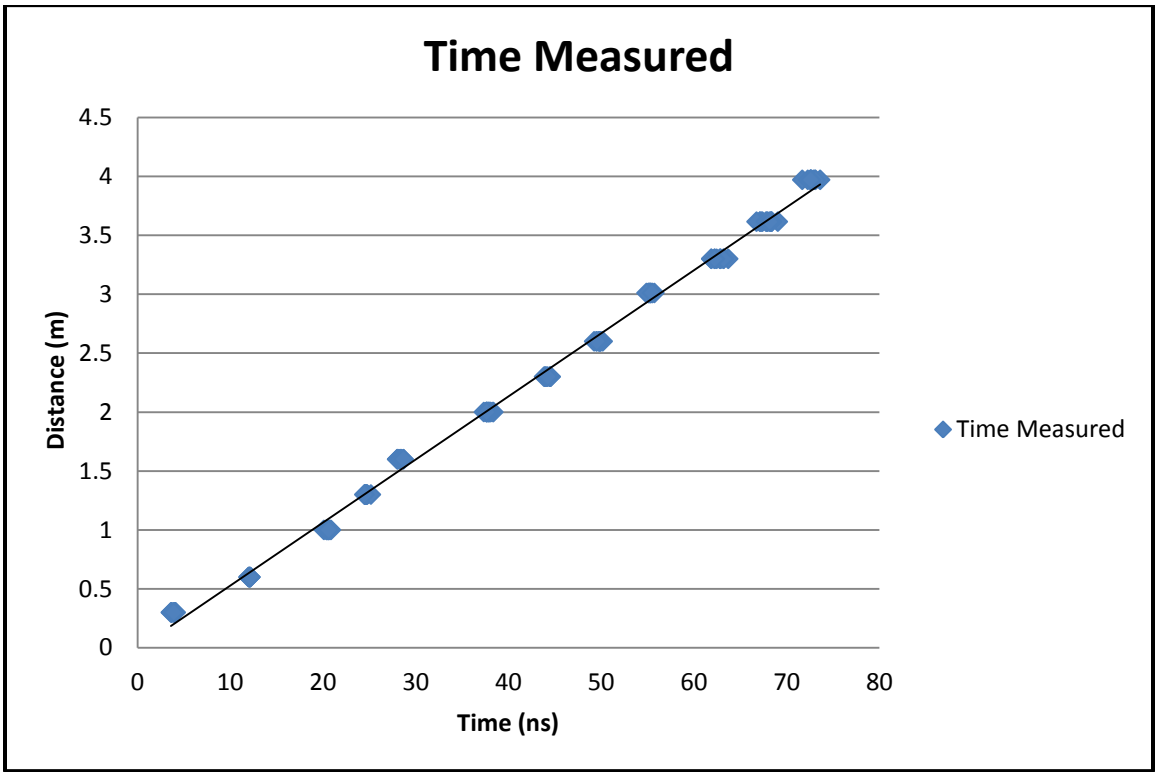

Figure 4.2 Time measured at different reference distances

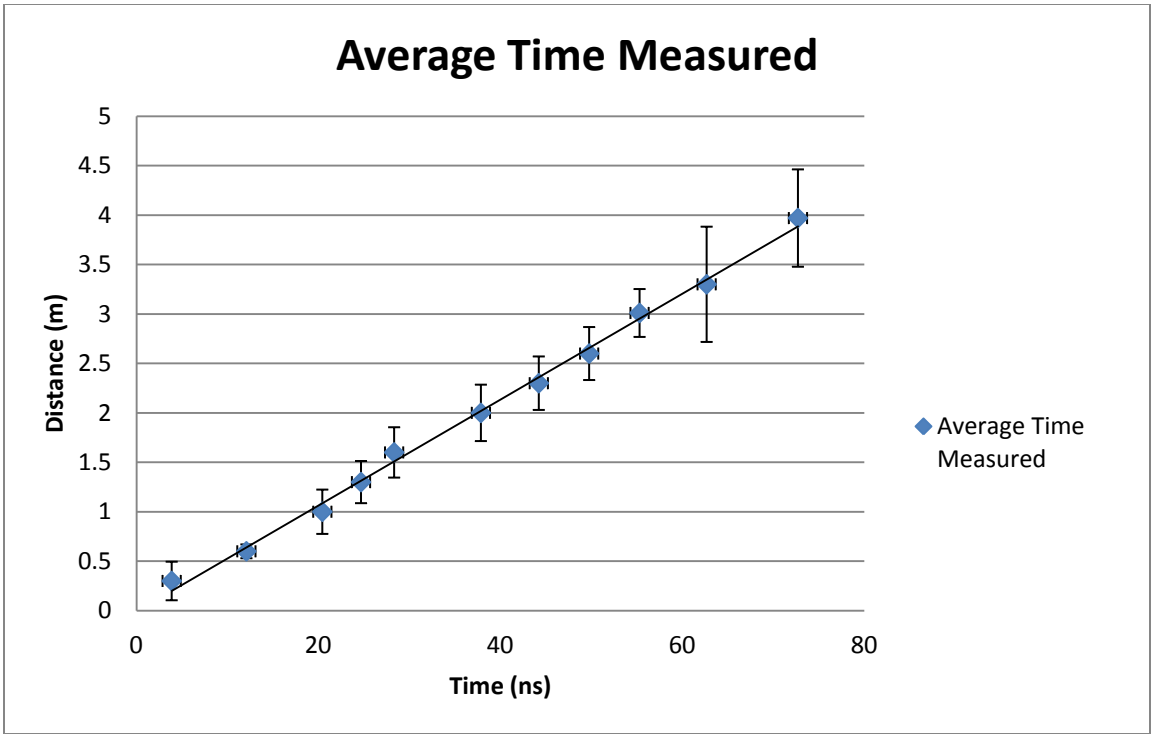

Figure 4.3 Average time measured at different reference distances

As can be seen from the figures above, the time increases linearly with distance as expected. The equation of the line, *distance= 0.0536*time-0.0081*, is used to calculate the distance using the ATMega128.

The problems with the current implementation are:

- The distance measured by the current system is affected by temperature changes in the environment.
- The error in the system increases with the increase in the distance measured.
- Not enough memory to compensated time errors by software.

Some improvement must be done to improve the current design. These improvements are described in the following section.

5. System Improvements and Conclusion

This section describes changes that will be done to the designed laser rangefinder in order to improve its accuracy and resolution. These changes will be done without increasing the size of the rangefinder and keeping the cost to a minimum.

5.1. Sending Channel Improvement

The minimum pulse width of the laser signal is 125ns with the ATMega128 running at 16MHz. The pulse width of this signal will be reduced to 80ns in order to increase the bandwidth of the system from 6MHz to around 88MHz. This bandwidth will be suitable for the receiver channel implemented using the OPA657.

To obtain shorter pulses, a faster microcontroller needs to be used. The ATMega128 microcontroller will be replaced by the PIC32MX795F512 from Microchip Technology Incorporated. This 32-bits microcontroller has a speed of 80MHz, an internal RAM of 512KB and a 64-TQFP

package which is smaller than the package of the ATMega128. Furthermore, free samples are available which will not add cost to the redesign.

Also, to help with the reduction on the size of the board and obtain a higher optical power, the 905D1S1.5U PLD will be replaced for the SPL LL90 PLD which has an integrated MOSFET and output peak power of 25W. The SPL LL90 can be drive using the EL7104 driver and will not require the use of the IRF840 MOSFET helping to reduce the board size. In addition, the SPL LL90 is half the price of the 905D1S1.5 and is currently available for the project.

5.2. Receiver Channel Improvement

The current implementation is strongly affected by the changes in temperature. At a constant bias voltage, the APD operating temperature affects its output current. This produces error of up to 2ns in the time measurement. This error can be seen when comparing the time measurements on figures 4.3 and 5.1.

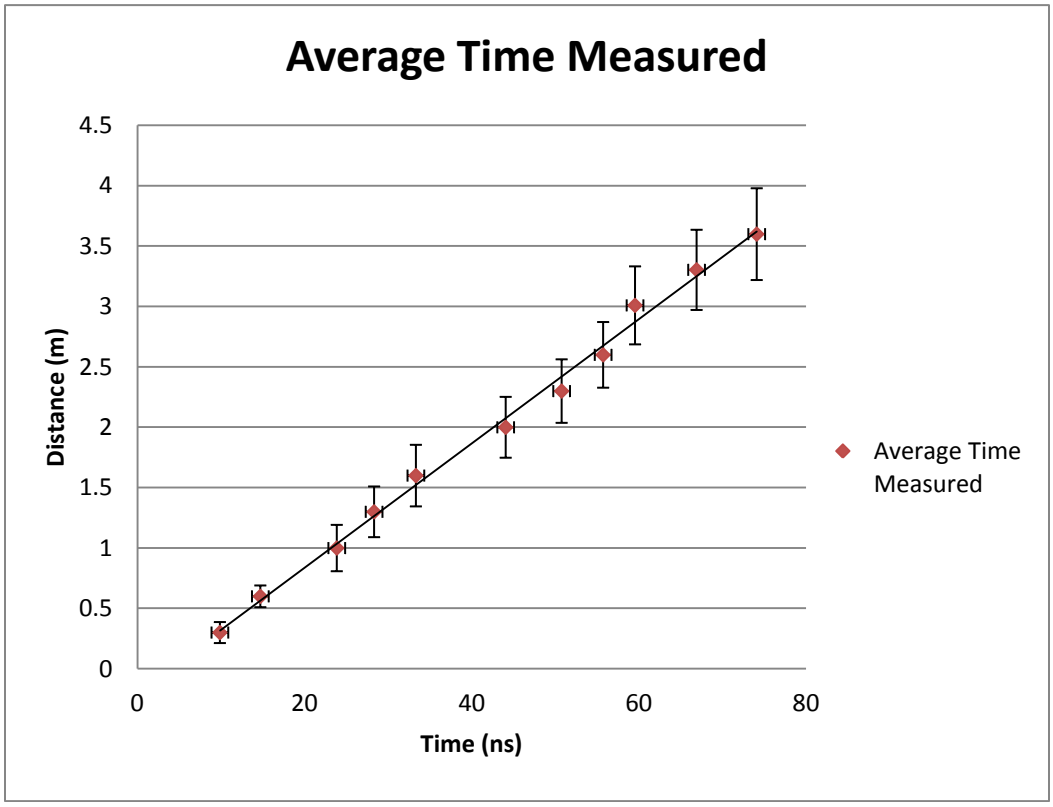

Figure 5.1 Averaged time measured at cooler temperature

There is a time different of up to 6ns between the times measured at cool and warn temperatures. For example, at a distance of 0.3-meters, the time shown on figure 4.3 is 3.8776ns while in figure 5.1 is 9.8732ns. Furthermore, at 1-meter, the time measured on figure 4.3 is 20.4353ns while in figure 5.1 is 23.858ns. The variations on temperature affect the accuracy and reliability of the laser rangefinder. Moreover, it is not possible to use the calculate distances and compensated for the error using in the laser using a time table.

A temperature controller must be added to the APD to reduce the effects of temperature. A thermoelectric controller (TEC) as shown on Figure 5 of [1] depicted below.

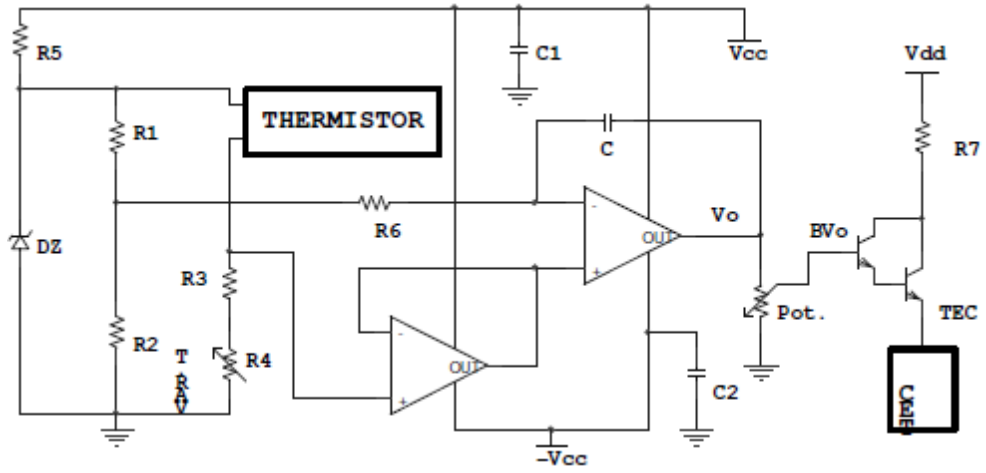

Figure 5.2 Thermoelectric Controller

The Thermistor is used to sense the temperature of the APD. Therefore, the Thermistor must be placed as closed as possible to the APD in order to ensure a minimal temperature gradient between the two devices. Adding this TEC circuit to the design will increase the power consumption and size of the board.

Instead of adding a TEC circuit to the design, the 0.4US5-P0.1 high voltage DC-DC converter will be replaced for a DC-DC converter with an integrated temperature controller. The dBC-380-5R from Laser Components, INC., is a high voltage module specially design for APD operation. It delivers a 380V output from a 5V input, and includes a temperature compensation circuit for the APD. In addition, the dBC-380-5R comes in a smaller package than the 0.4US5-P0.1, and can supply a higher output current. Also, the dBC-380-5R provides RS232 interface to regulate the bias voltage of the APD.

In addition, a new TDC will be used. The TDC-GP1 will be replaced for the TDC-GP2 because the last mentioned has a higher resolution and smaller package size. The resolution of the GP2 is 65ps which is equivalent to around 1cm in distance, and comes in a QFN32 package. Furthermore, the GP2 has a lower power consumption when compare to the GP1, and has a 4-wire SPI-Interface that helps to reduce the number of connection between the TDC and the microcontroller. Replacing the GP1 for the GP2 will improve the resolution of the system; reduce its power consumption and size.

Moreover, the LT1394 comparator will be replaced for the LT1720 comparator. The LT1720 has a propagation delay of 4.5ns which helps to reduce the propagation delay of the received signal. The LT720 is a dual-comparator which can be operate using a single 5V supply and its voltage range is from -0.1V to 3.8V. The LT1720 comes in the same package as the LT1394, and free-samples are available.

Using the LT1720 comparator will allow reducing the walk-error of the signal by using the method in [4] and [5]. The compensation technique describe in [4] and [5] utilizes the TDC to measure the slew-rate of the front edge of the pulse using two comparators with two different thresholds resulting in two timing marks for the GP2, and then using the known relationship of the walk and signal-ratio to compensate for the walk-error. This principle is shown on figure 4 of [4] shown below.

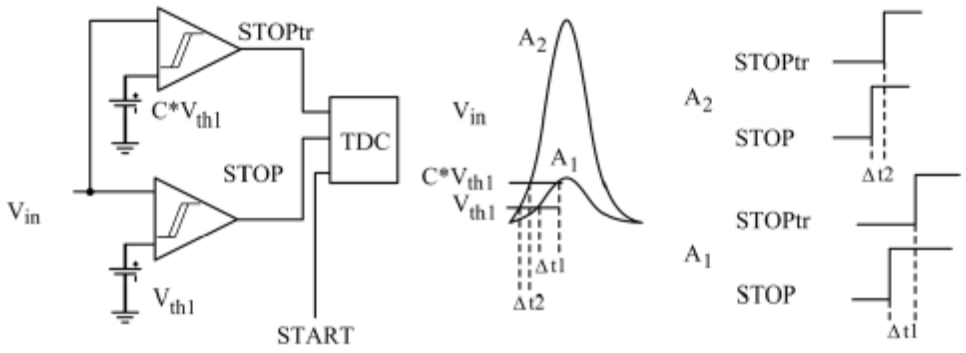

Figure 5.3 Principle of time domain compensation

This method takes advantages of the on board TDC. Like the GP1, the GP2 has one start channel and two-stop channels. These channels will be used to measure the slew-rate of the received signal and a table look-up will be used to further reduce the walk error. Also, the OPA657 will be change from a SOIC package to a SOT-23 package without the addition of any cost.

5.3. Conclusion

This thesis addresses the design and implementation of a pulsed laser rangefinder using the time-of-flight principle. The implemented system uses a pulsed laser diode and a laser driver to send a light pulse toward a measurement target; an avalanche photodiode and signal amplifiers to photo-electrically convert and amplify the reflected light of the target; a TDC to measure the delay time of the light signal; and a microprocessor to send the driving signal to the pulsed laser diode driver, send the start counter signal to the TDC, read the time information from it and calculate the distance.

The rise time of the driver signal for the PLD is 58ns which gives a system bandwidth of around 6MHz. The noise measured at the output of the amplifying channel was 50mV. The maximum output signal of the receiver channel is 4V which gives a signal-to-noise ratio (SNR) of 80. Knowing these values, according to equation 2 of [8], the single-shot resolution for the system is approximately 10cm. The resolution is improve by averaging of 100 measurements [8, equation 3] to 1cm for distances of less than 1m. The resolution of the system deteriorates with increasing distance.

The total accuracy of the laser rangefinder is affected by the walk error of the receiver channel and the changes in the room temperature. Also, the noise at the output of the receiver channel limits the minimum detectable signal. Some improvements need to be done to the system to improve its accuracy and speed. These improvements are explained in the previous sections. They will allow the expandability of the current system to a scanning laser rangefinder without the need of major changes.

Bibliography:

[1] Mohammad, Nejad S., and Olyaee, S., "Unified Pulsed Laser Range Finder and Velocimeter Using Ultra-Fast Time-To-Digital Converter." *Iranian Journal of Electrical & Electronic Engineering.,* Vol. 5, No. 2, pp. 112-21, 2009.

[2] Intersil application note 118. "Applying Power MOSFET Drivers." http://www.nalanda.nitc.ac.in/industry/appnotes/Elantec/d40931.pdf

[3] Palojarvi, P.; Ruotsalainen, T.; Kostamovaara, J.; , "A 250-MHz BiCMOS receiver channel with leading edge timing discriminator for a pulsed time-of-flight laser rangefinder," *Solid-State Circuits, IEEE Journal of* , vol.40, no.6, pp. 1341- 1349, June 2005

[4] Nissinen, J.; Kostamovaara, J., "A 0.13 µm CMOS laser radar receiver with leading edge detection and time domain error compensation," *Instrumentation and Measurement Technology Conference, 2009. I2MTC '09. IEEE* , vol., no., pp.900-903, 5-7 May 2009

[5] Nissinen, J.; Nissinen, I.; Kostamovaara, J., "Integrated Receiver Including Both Receiver Channel and TDC for a Pulsed Time-of-Flight Laser Rangefinder With cm-Level Accuracy," *Solid-State Circuits, IEEE Journal of*, vol.44, no.5, pp.1486-1497, May 2009

[6] Kelly, Alonzo. "Concept Design of a Scanning Laser Rangefinder for Autonomous Vehicle," 8 May, 1997. The Robotics Institute, Carnegie Mellon University. 10 September, 2011. <http://www.frc.ri.cmu.edu/~alonzo/pubs/reports/rangefinder.pdf>.

[7] Mohammad Nejad S. and Olyaee S., "Low-noise high-accuracy TOF laser range finder", *Am. J. Appl. Sci*., Vol. 5, No. 7, pp. 755-762, 2008.

[8] Ruotsalainen, T.; Palojarvi, P.; Peltola, T.; Kostamovaara, J., "A low-noise receiver channel for a pulsed laser rangefinder," *Circuits and Systems, 1997. Proceedings of the 40th Midwest Symposium on* , vol.2, no., pp. 1395- 1398 vol.2, 3-6 Aug. 1997

[9] Williams, Jim, "Signal Sources, Conditioners and Power Circuitry," Linear Technology Corporation, Application Note 98, November 2004, p. 20-21.

[10] "SARF500 - Silicon Avalanche Photodiode with Integrated Band-pass Filter," Laser Components USA, INC. Web. 23 February 2012. <http://www.lasercomponents.com/us/product/silicon-avalanche-photodiodes/>.

[11]" OPA656 - Wideband, Unity Gain Stable FET-Input Operational Amplifier." Texas Instruments INC. Web. 18 May 2012. <http://www.ti.com/product/opa656>.

[12] "OPA657 - 1.6GHz, Low Noise, FET -Input Operational Amplifier." Texas Instruments INC. Web. 18 May 2012. <http://www.ti.com/product/opa657>.

[13] "OPA846 - Wideband, Low Noise, Voltage Feedback Operational Amplifier." Texas Instruments INC. Web. 18 May 2012. <http://www.ti.com/product/opa846>.

[14] "ATmega128- 8-bit Atmel Microcontroller with 128Kbytes In-System Programmable Flash." Atmel Corporation. Web. 18 May 2012. <http://www.atmel.com/devices/atmega128.aspx>.

[15] “TDC-GP1 Multihit Time-to-Digital Converter 2-channel TDC." Transducer Direct, LCC. Web. 18 May 2012. <http://www.acam-usa.com/GP1.html>.

[16] Ramus, Xavier. "Transimpedance Considerations for High-Speed Operational Amplifiers.” Application *Report - SBOA122.* Texas Instruments INC, 22 Nov. 2009. Web. 18 May 2012. <http://www.ti.com/general/docs/litabsmultiplefilelist.tsp?literatureNumber=sboa122>.

[17] Blake, Kumen, and Bible, Steven. "Amplifying High-Impedence Sensors - Photodiode Example.Microchip Technology INC, 25 July 2006. Web. 18 May 2012. <http://www.microchip.com/stellent/idcplg?IdcService=SS_GET_PAGE&nodeId=1824&appnote=en021228>.

[18] Nissinen, I.; Mantyniemi, A.; Kostamovaara, J., "A CMOS time-to-digital converter based on a ring oscillator for a laser radar," *Solid-State Circuits Conference, 2003. ESSCIRC '03. Proceedings of the 29th European*, vol., no., pp.469-472, 16-18 Sept. 2003.